GWs FROM COALESCING BINARIES
RESULTS AND FUTURE PERSPECTIVES

Gianluca Gemme
INFN Sezione di Genova

Credits: A. Buonanno, W. Del Pozzo, M. Favata, J. van den Brand and many others…

Università degli Studi di Cagliari, Dipartimento di Fisica, 18 giugno 2018

GRAVITATIONAL DETECTOR NETWORK

Scientific runs

O1: 12 Sep 2015 → 19 Jan 2016

O2: 30 Nov 2017 → 25 Aug 2017 (Virgo: 1 Aug 2017 → 25 Aug 2017)

LIGO-Virgo

ADVANCED VIRGO

6 European countries
23 labs, ~280 authors

Advanced Virgo (AdV): upgrade of the Virgo interferometric detector

Participated by France and Italy (former founders of Virgo), The Netherlands, Poland, Hungary, Spain

Funding approved in Dec 2009
(21.8 ME + Nikhef in kind contribution)

Project formally completed with the start of the O2 run (1 Aug 2017)

APC Paris
ARTEMIS Nice
EGO Cascina
INFN Firenze-Urbino
INFN Genova
INFN MiB-Parma-Torino
INFN Napoli
INFN Perugia
INFN Pisa
INFN Roma La Sapienza
INFN Roma Tor Vergata
INFN Padova
INFN Salerno/Uni Sannio
INFN TIFPA Trento
LAL Orsay – ESPCI Paris
LAPP Annecy
LKB Paris
LMA Lyon
NIKHEF Amsterdam
POLGRAW
RADBOUD Uni. Nijmegen
RMKI Budapest
University of Valencia

ADVANCED VIRGO DESIGN

Advanced Virgo started operation on August 1, 2017. It features many improvements with respect to Virgo and Virgo+

For 2017

- Larger beam: 2.5x larger at ITMs
- Heavier mirrors: 2x heavier
- Higher quality optics: residual roughness < 0.5 nm
- Improved coatings for lower losses: absorption < 0.5 ppm, scattering < 10 ppm
- Reducing shot noise: arm finesse of cavities are 3 x larger than in Virgo+
- Thermal control of aberrations: compensate for cold and hot defects on the core optics:
  - ring heaters
  - double axicon CO2 actuators
  - CO2 central heating
  - diagnostics: Hartmann sensors & phase cameras
- Stray light control: suspended optical benches in vacuum, and new set of baffles and diaphragms to catch diffuse light
- Improved vacuum: 10^{-9} mbar instead of 10^{-7} mbar

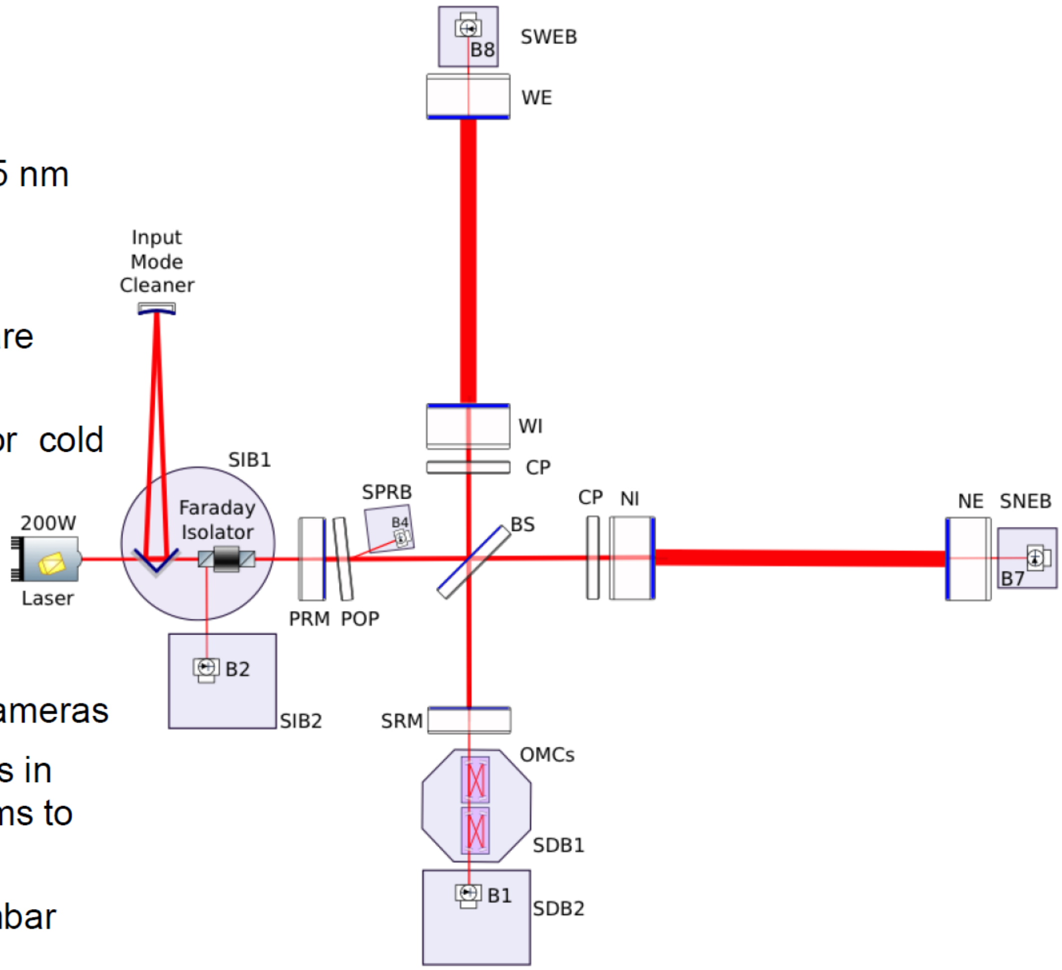

Class. Quantum Grav. 32 (2015) 024001

O2 SUMMARY

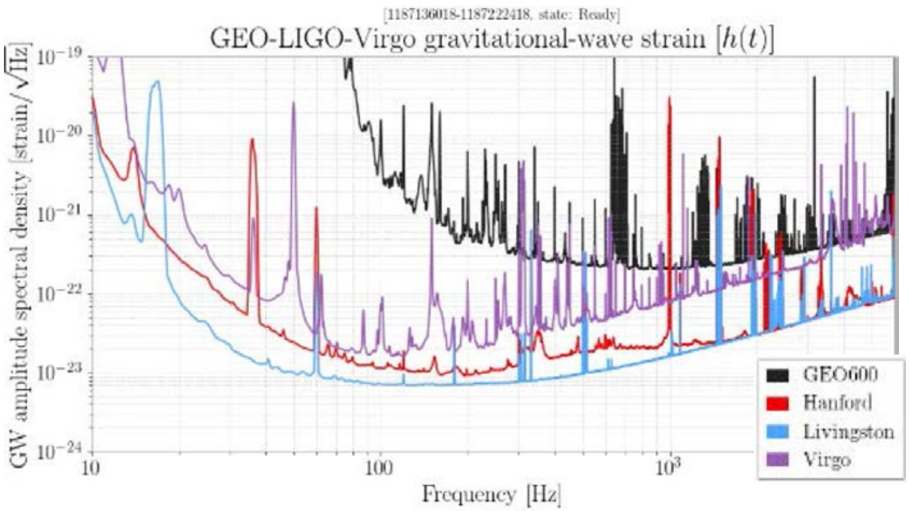

Noise budget

Many bumps and lines and some extra broadband noise

Scattered light, some sensing noise, unknown….

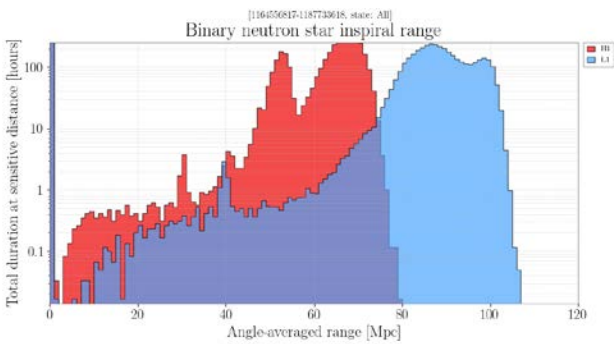

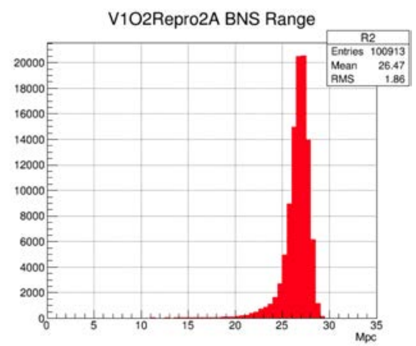

VIRGO

HIGHEST BNS RANGE: **28.2 Mpc**

AVERAGE RANGE:

BNS 26 - BBH$_{10}$ 134 - BBH$_{30}$ 314 Mpc

DUTY CYCLE: **85%**

LONGEST LOCK STRETCH: **69 hrs**

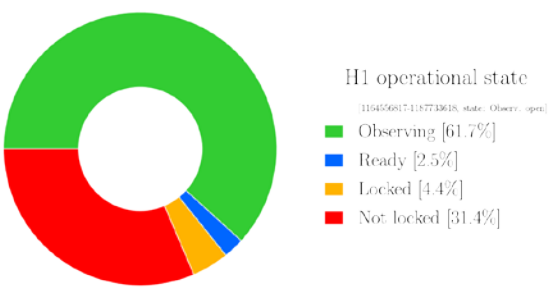

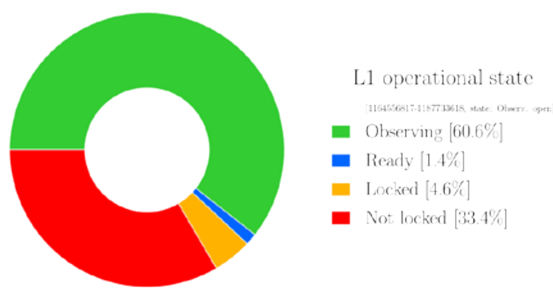

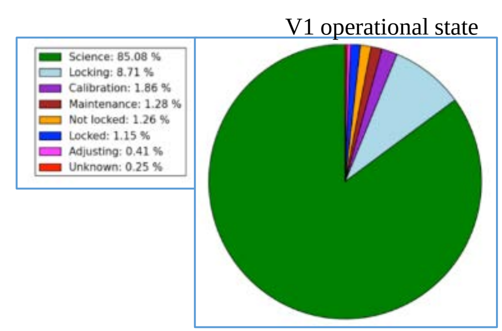

O2 DETECTIONS

GW170104

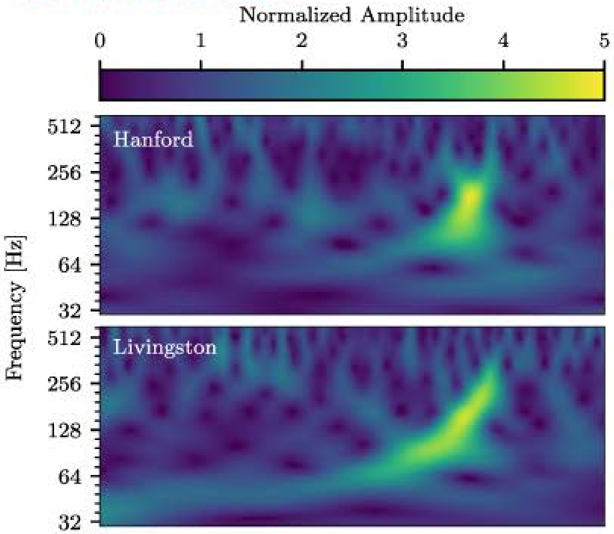

GW170608

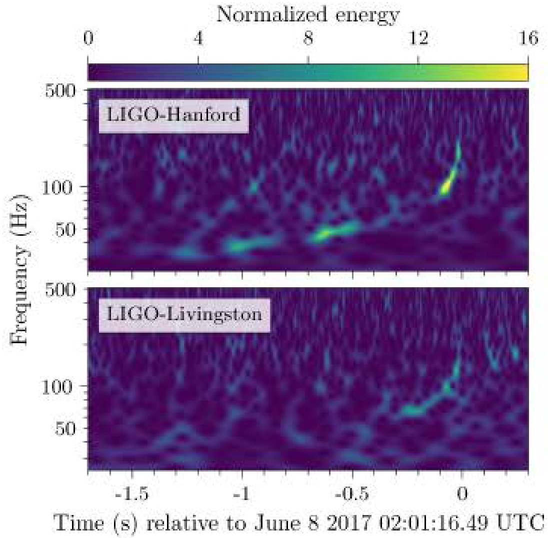

GW170817

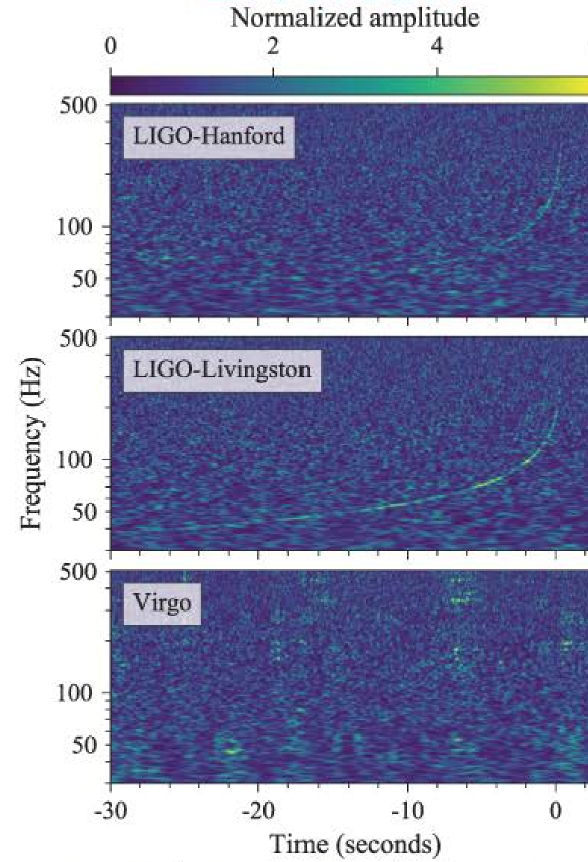

GW170814

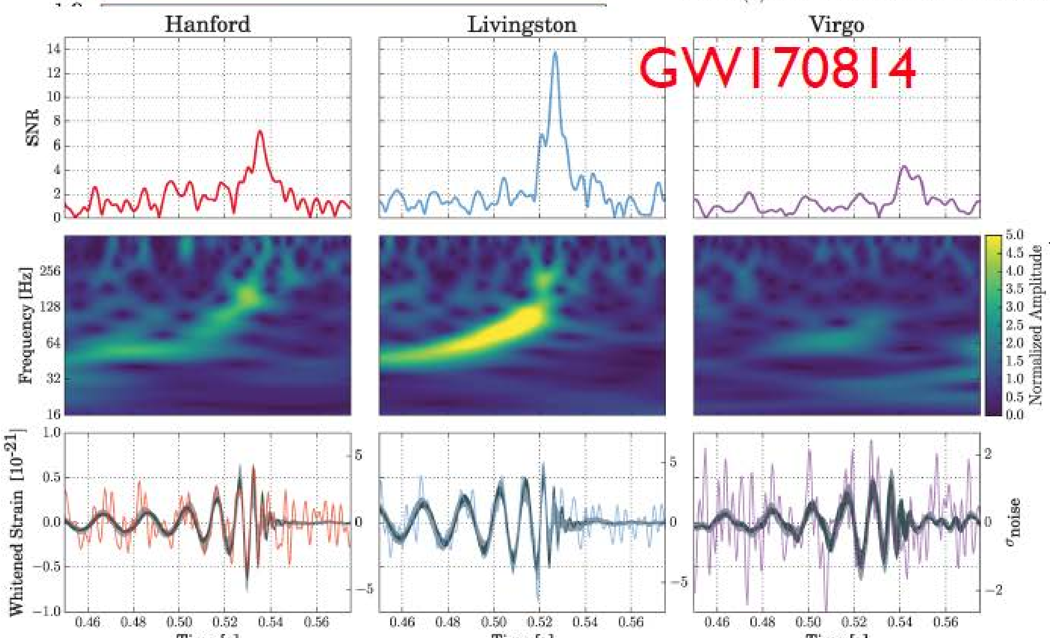

Source	SNR	M $(M_\odot)$	d_L (Mpc)
GW150914	23.7	65.3	420
LVT151012	9.7	37	1000
GW151226	12.0	21.8	440
GW170104	13.0	50.7	880
GW170608	13	19	340
GW170814	18.3	55.9	540
GW170817	32.4	2.74	40

LESSONS LEARNED…

…and open questions

GW FROM COMPACT BINARIES

Compact binaries are the preferred sources for GW detectors

The GW signal from CB is divided into three stages: **inspiral, merger and ringdown**

Inspiral: **Post-Newtonian theory**
Sensitive to GW back-reaction, spin-orbit, spin-spin couplings, …

Merger: **numerical GR**

Ringdown: **BH perturbation theory**: end-product relaxes to a stationary state

- **damped sinusoids**
- Parametrized IMR waveforms (pEOBNR)

*Abbott et al. (LIGO Collaboration, Virgo Collaboration), Phys. Rev. Lett. **116**, 061102 (2016)*

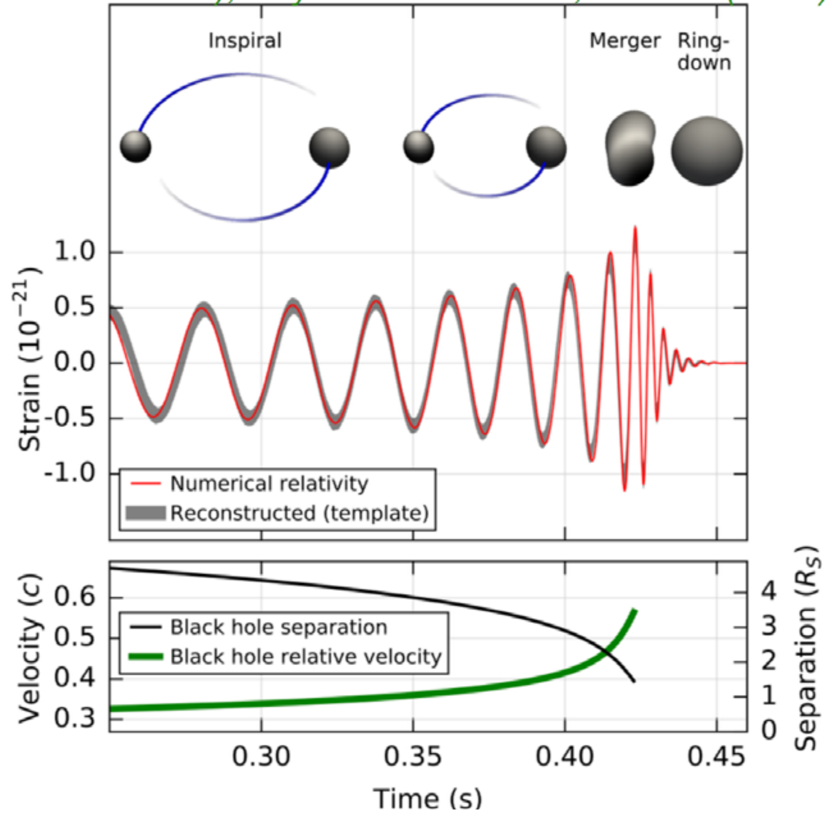

INSPIRAL

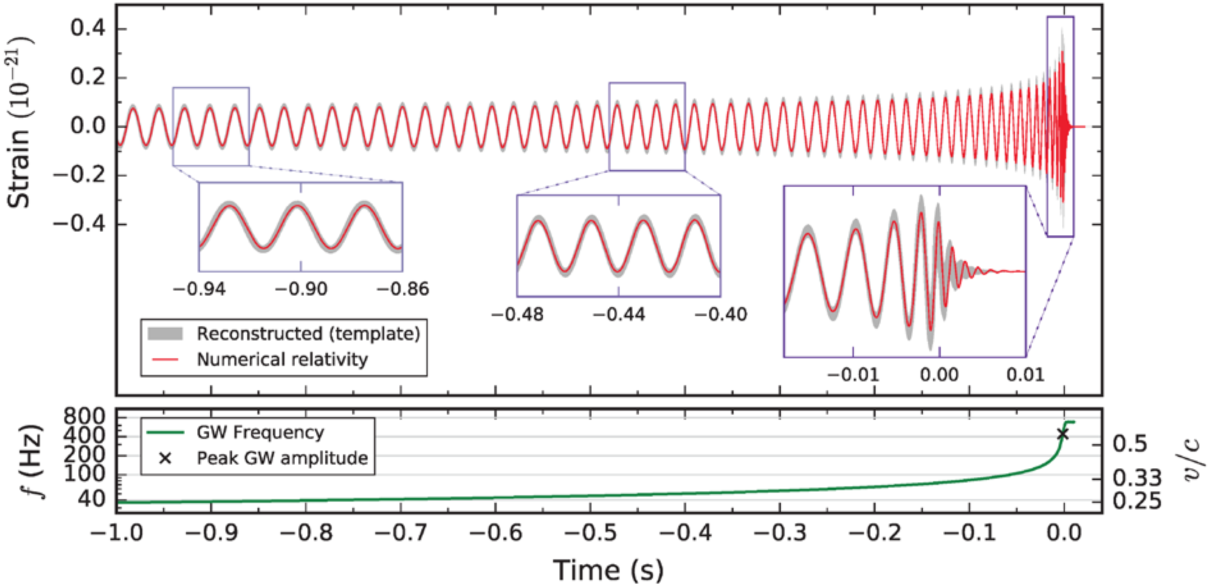

$$h(t) = F_+(\theta, \phi, \psi)\, h_+(t, \iota) + F_\times(\theta, \phi, \psi)\, h_\times(t, \iota)$$

Amplitude (circular orbit, leading-orer)

$$h_+ \propto \mathcal{F}(\iota)\, \frac{\mathcal{M}^{5/3}}{d_L}\, f_{GW}^{2/3} \cos\left(2\pi f_{GW}\, t + 2\Phi_0\right) \qquad \mathcal{M} = \eta^{3/5} M = \left(\frac{\mu}{M}\right)^{3/5} M$$

Post-newtonian expansion $\dfrac{dE_{GW}}{dt} + \dfrac{dE_{orb}}{dt} = \dfrac{dE_{GW}}{dt} + \dfrac{dE_{orb}}{df_{GW}} \dfrac{df_{GW}}{dt} = 0$

$$\frac{df_{GW}}{dt} \propto \mathcal{M}^{5/3} f_{GW}^{11/3} \left[1 + a_{1PN}(\eta)\left(\pi M f_{GW}\right)^{2/3} + a_{1.5PN}(\eta, \chi)\left(\pi M f_{GW}\right) + \cdots\right]$$

TERMINATION FREQUENCY

Ending frequency sets the total mass:

$$f_{GW,end} \sim \frac{1}{M}$$

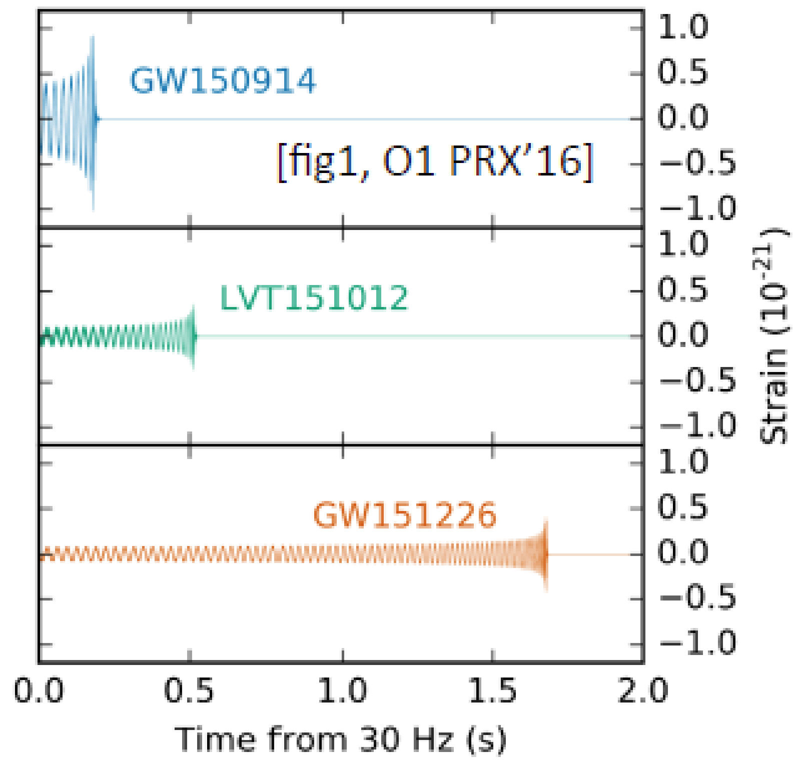

Innermost stable circular orbit (ISCO)

$$r_{ISCO} = \frac{6GM}{c^2}$$ (Schwarzschild background)

$$\omega_{s,end}^2 = (\pi f_{GW,end})^2 = \frac{GM}{r_{ISCO}^3}$$ (Kepler's law)

$$f_{GW,max} = \frac{1}{6\sqrt{6}\,(2\pi)}\frac{c^3}{GM} \simeq 2.2\,\mathrm{kHz}\left(\frac{M_\odot}{M}\right)$$

SIGNAL DURATION AND RADIATED ENERGY

Smaller mass, smaller mass ratio, smaller chirp mass → longer signal duration, more cycles

$$\mathcal{N}_{cycles} = \frac{1}{32\pi^{8/3}}\left(\frac{G\mathcal{M}}{c^3}\right)^{-5/3}\left(f_{min}^{-5/3} - f_{max}^{-5/3}\right) \simeq 2.6\times 10^3\left(\frac{30\,\mathrm{Hz}}{f_{min}}\right)^{5/3}\left(\frac{1.2M_\odot}{\mathcal{M}}\right)$$

In Newtonian approximation

$$\frac{dE}{df} = \frac{\pi^{2/3}}{3G}(G\mathcal{M})^{5/3} f_{max}^{2/3}$$

$$\Delta E_{rad} = \frac{\pi^{2/3}}{2G}(G\mathcal{M})^{5/3} f_{max}^{2/3} \simeq 4.2\times 10^{-2} M_\odot c^2\left(\frac{\mathcal{M}}{1.21M_\odot}\right)^{5/3}\left(\frac{f_{max}}{1\,\mathrm{kHz}}\right)^{2/3}$$

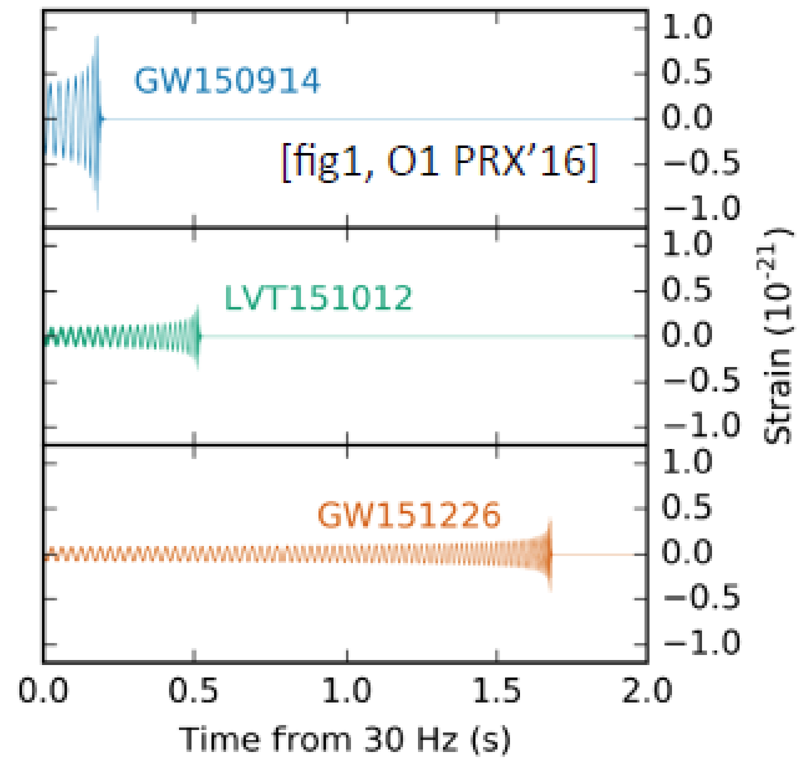

MASSES

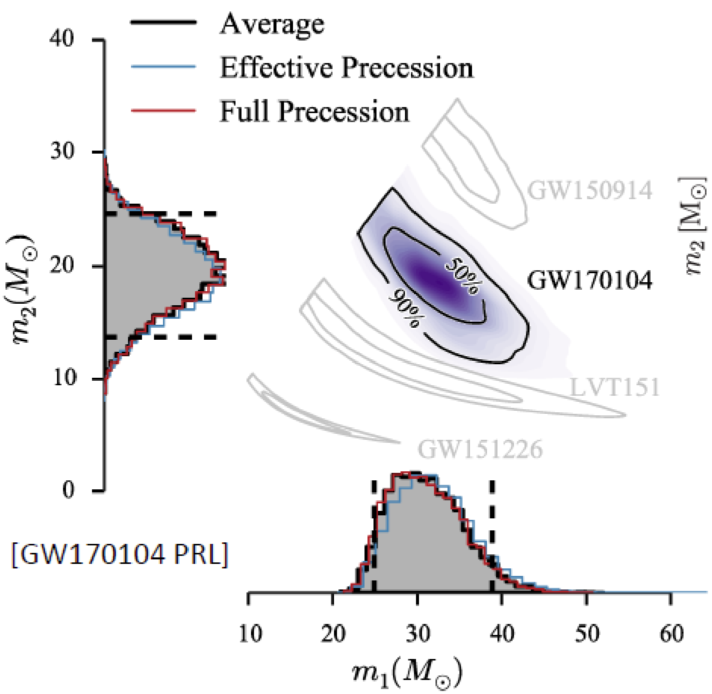

[GW170104 PRL]

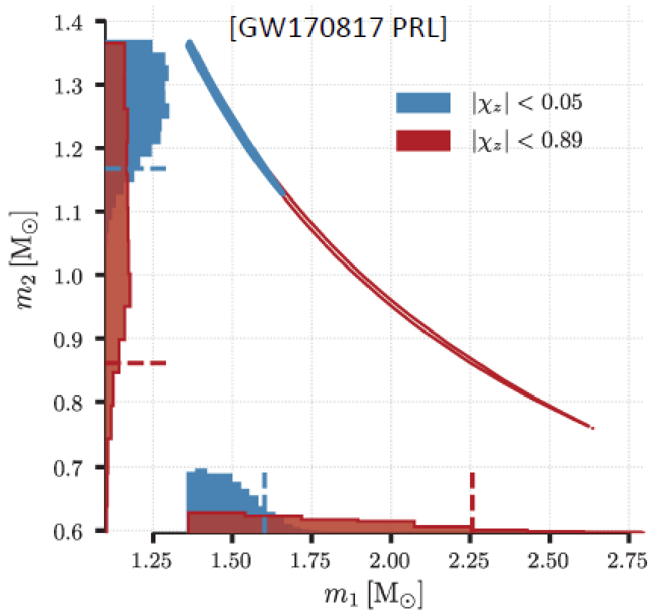

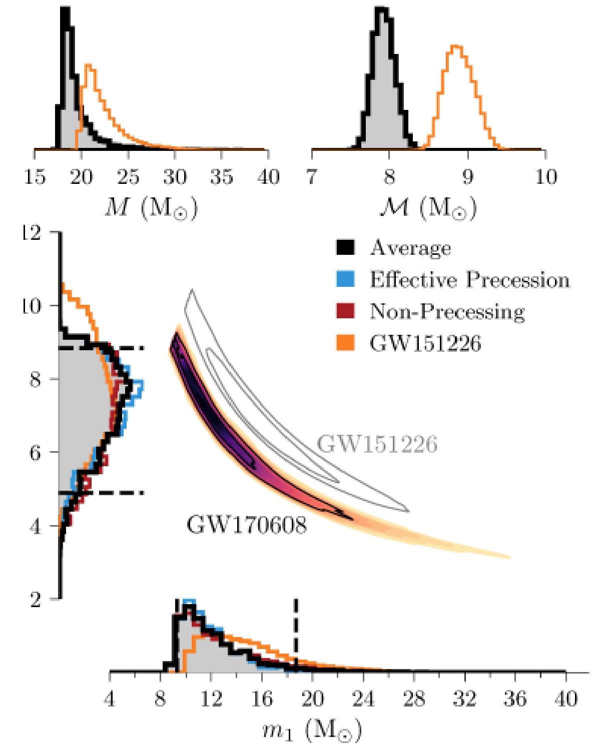

[GW170608, submitted]

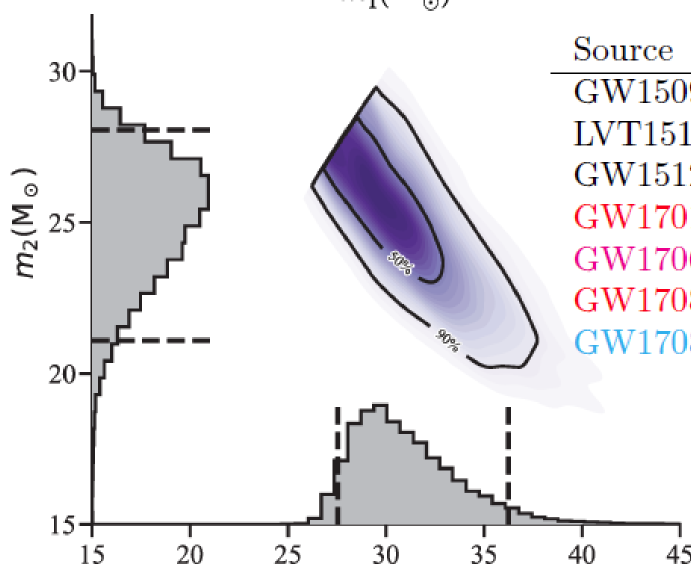

[GW170814 PRL]

Source	SNR	$M/M_\odot$	$\delta M/M$	$\mathcal{M}_{ch}/M_\odot$	$\delta\mathcal{M}_{ch}/\mathcal{M}_{ch}$	$m_1/M_\odot$	$m_2/M_\odot$
GW150914	23.7	65.3	0.058	28.1	0.060	36.2	29.1
LVT151012	9.7	37	0.23	15.1	0.086	23	13
GW151226	12.0	21.8	0.17	8.9	0.034	14.2	7.5
GW170104	13.0	50.7	0.11	21.1	0.12	31.2	19.4
GW170608	13	19	0.16	7.9	0.025	12	7
GW170814	18.3	55.9	0.055	24.1	0.054	30.5	25.3
GW170817	32.4	2.74	0.011	1.188	0.0025	1.36	1.17

$$\text{frac. error in mass parameters} \sim \frac{1}{\text{SNR} \times \text{N}_{\text{cycles}}}$$

[Fractional errors in above table estimated from ½ the 90% confidence interval; other numbers from published/submitted LSC papers.]

SPINS

Phase corrections dominated by ``effective spin parameter''

$$\pi \frac{df_{\rm gw}}{dt} = \frac{96}{5}\pi^{11/3}\mathcal{M}_{\rm ch}^{5/3} f_{\rm gw}^{11/3}\Big[1 + a_{1\rm PN}(\eta)(\pi M f_{\rm gw})^{2/3} + a_{1.5\rm PN}(\eta, \chi_{\rm eff})(\pi M f_{\rm gw}) + a_{2\rm PN}(\eta, \mathbf{S}_1, \mathbf{S}_2, Q_{\rm qm})(\pi M f_{\rm gw})^{4/3} + \cdots\Big]$$

$$\chi_{\rm eff} = \frac{1}{M}(m_1\chi_1 \hat{\mathbf{S}}_1 \cdot \hat{\mathbf{L}} + m_2 \chi_2 \hat{\mathbf{S}}_2 \cdot \hat{\mathbf{L}})$$

Precession arises only if there are spin-components in the orbital plane. This affects the amplitude (and the phase).

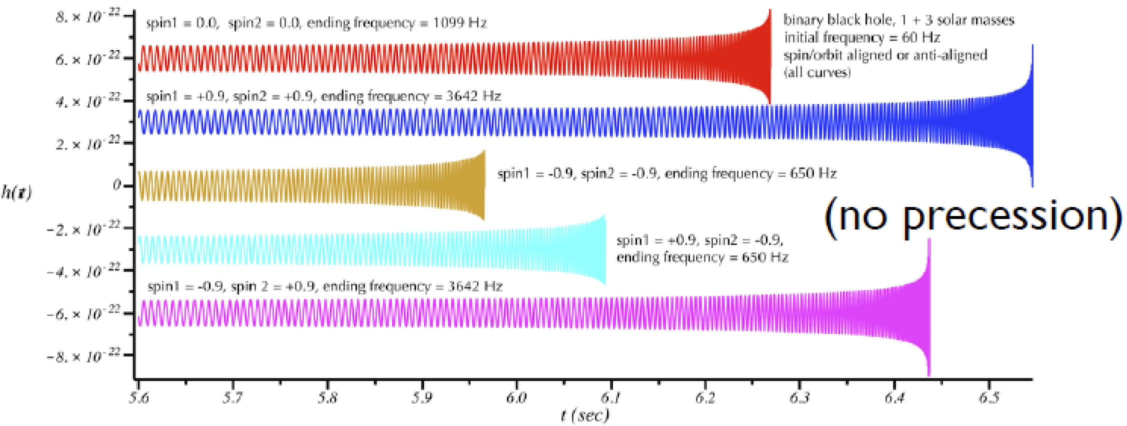

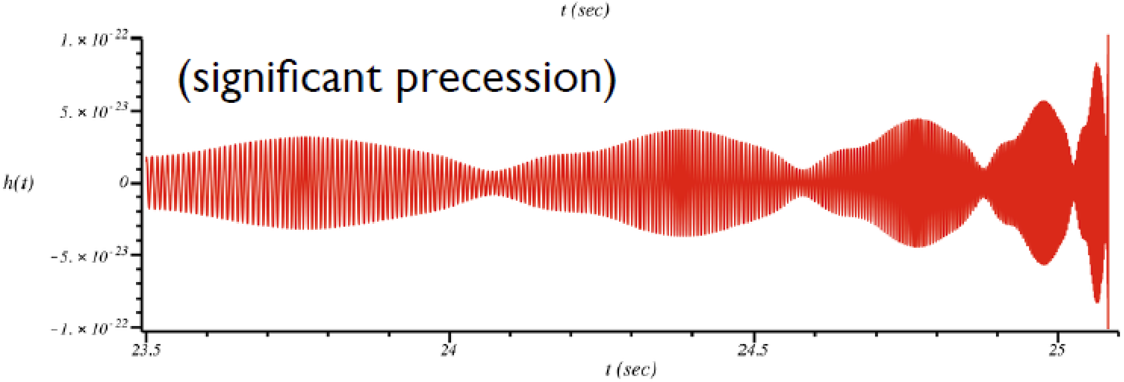

$$\frac{d\mathbf{S}_1}{dt} = \mathbf{\Omega}_1 \times \mathbf{S}_1$$

$$\frac{d\mathbf{S}_2}{dt} = \mathbf{\Omega}_2 \times \mathbf{S}_2$$

$$\frac{d\mathbf{L}}{dt} \approx -\left(\frac{d\mathbf{S}_1}{dt} + \frac{d\mathbf{S}_2}{dt}\right)$$

$$\cos\iota = \mathbf{L} \cdot \hat{\mathbf{N}}$$

SPINS

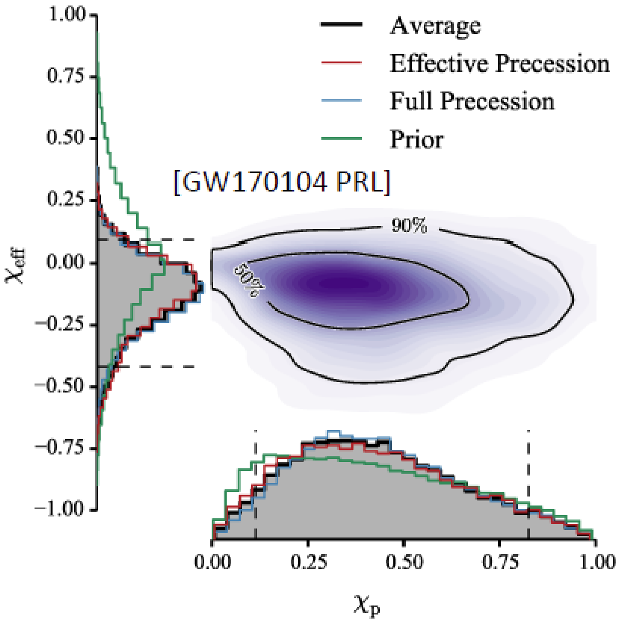

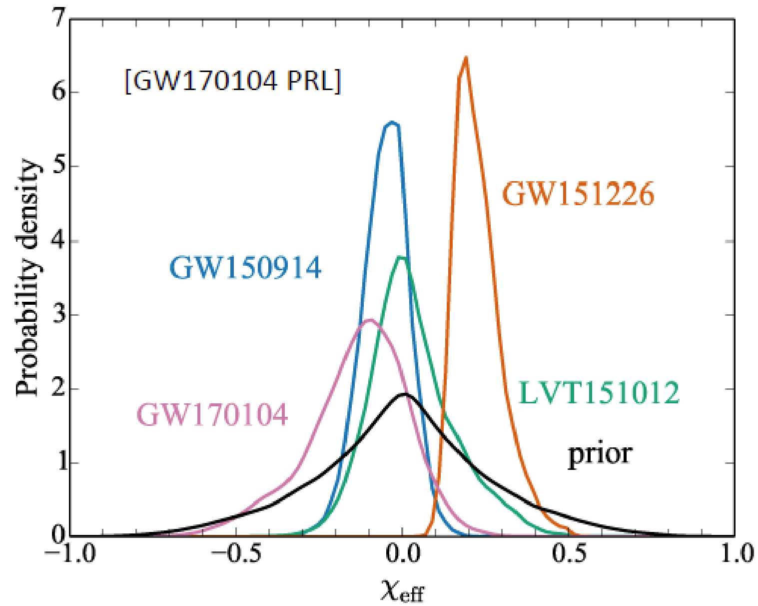

In-plane-spin components poorly constrained.

Weak constraints on effective spin.

Only GW151226 shows clear evidence for spin.

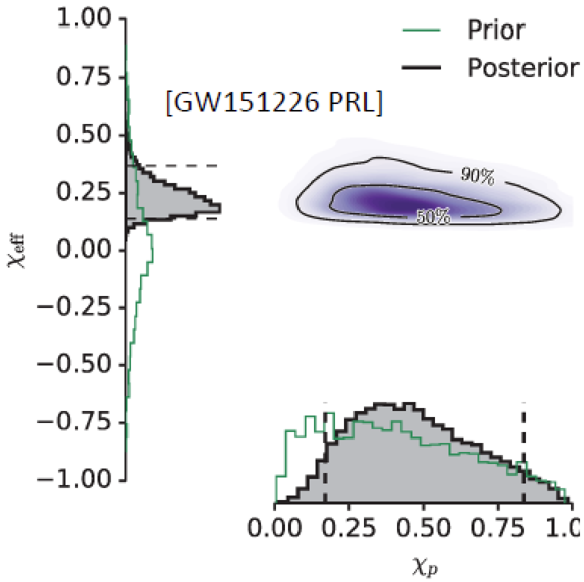

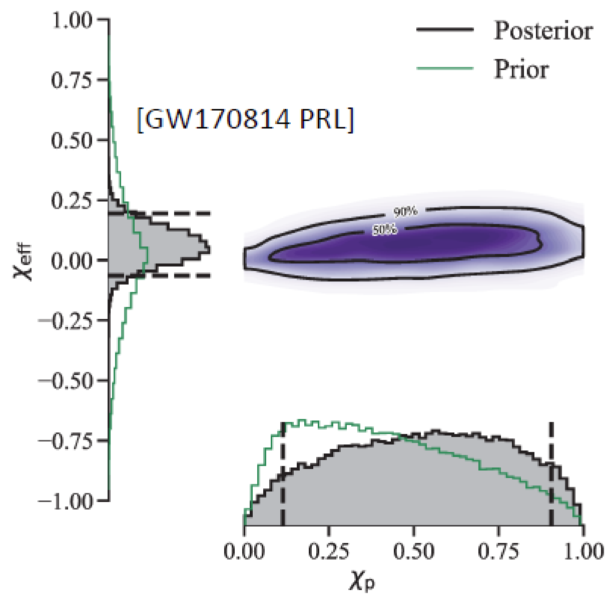

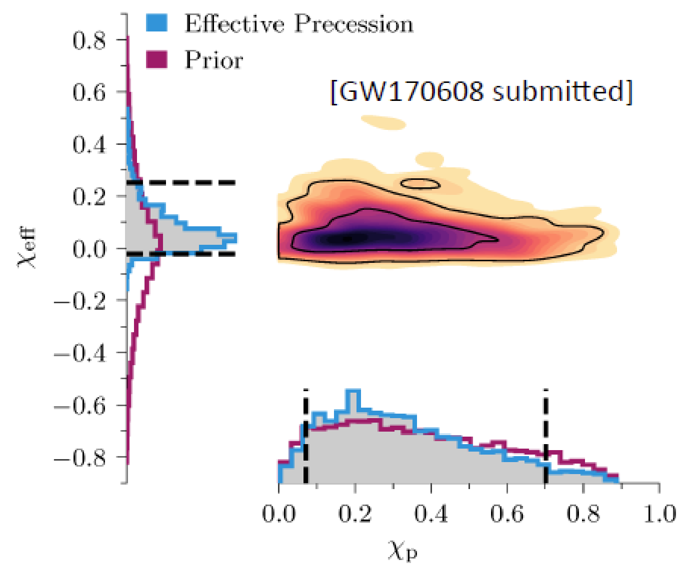

RINGDOWN

- Equation of **gravitational perturbations** in black-hole spacetime:

(Regge & Wheeler 56, Zerilli 70, Teukolsky 72)

$$\frac{\partial^2 \Psi}{\partial t^2} - \frac{\partial^2 \Psi}{\partial r_\star^2} + V_{\ell m} \Psi = 0$$

(Vishveshwara 70, Press 71, Chandrasekhar et al. 75)

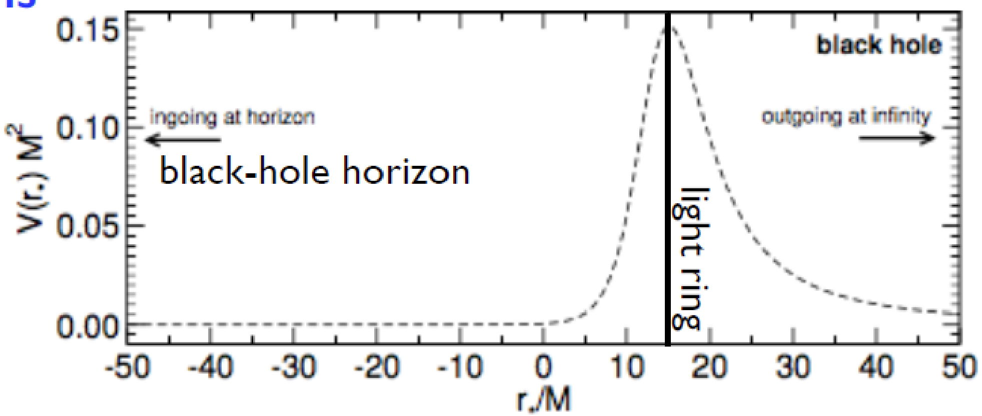

- If black-hole's size is $R_{\rm BH} = 2GM/c^2$ and mass $M = 20 M_\odot \Rightarrow R_{\rm BH} \sim 60\,{\rm km}$ **travel time of spacetime vibration** $\Rightarrow R_{\rm BH}/c \sim 0.2\,{\rm msec}$.
- For **each (l,m)**, infinite tower of **overtones n**.
- For astrophysical black holes (zero charge), QNM's **frequency** and **decay time** only depend on **mass and spin**.

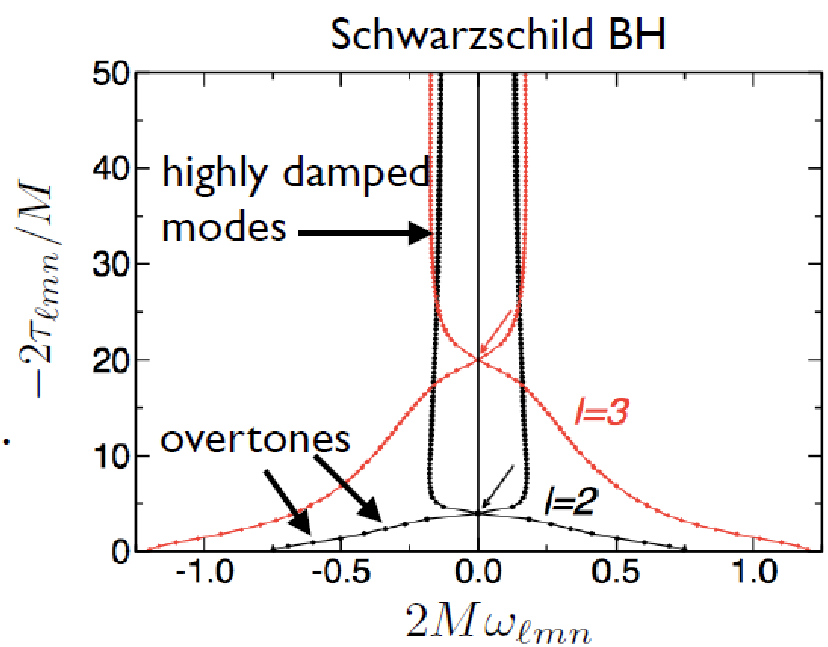

RINGDOWN

- Equation of gravitational perturbations in black-hole spacetime:

(Regge & Wheeler 56, Zerilli 70, Teukolsky 72)

$$\frac{\partial^2 \Psi}{\partial t^2} - \frac{\partial^2 \Psi}{\partial r_\star^2} + V_{\ell m} \Psi = 0$$

(Vishveshwara 70, Press 71, Chandrasekhar et al. 75)

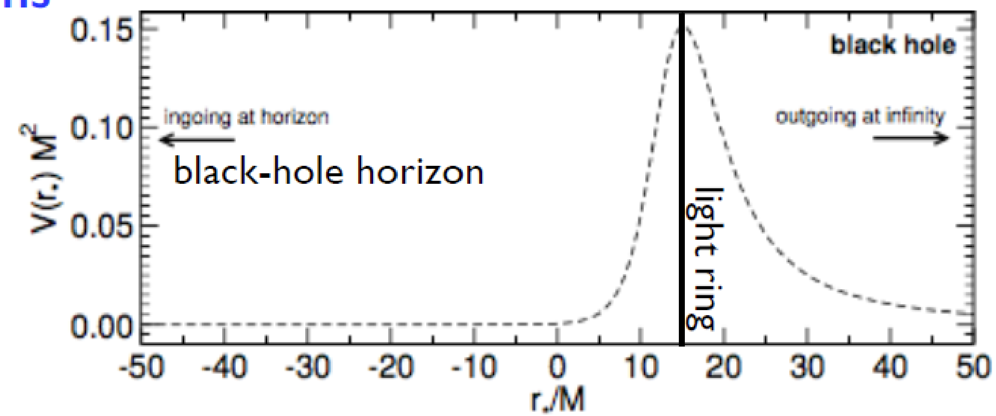

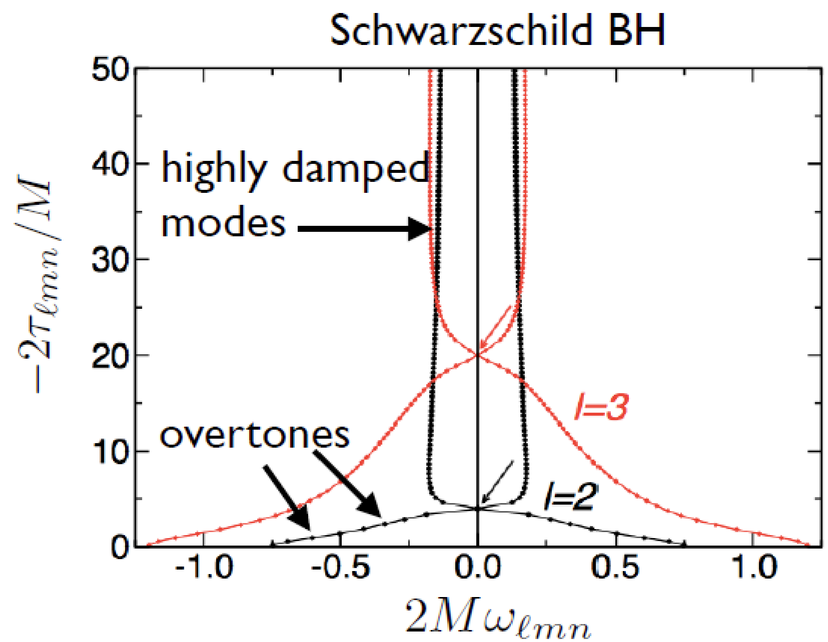

- For Schwarzschild BH of $M = 20 M_\odot$

$$f_{2m0} = 604\,\mathrm{Hz}, \tau_{2m0} = 1.10\,\mathrm{msec}$$
$$f_{2m1} = 560\,\mathrm{Hz}, \tau_{2m1} = 0.36\,\mathrm{msec}$$
$$f_{2m2} = 486\,\mathrm{Hz}, \tau_{2m2} = 0.20\,\mathrm{msec}$$

EFFECTIVE-ONE-BODY WAVEFORMS

- Evolve **two-body dynamics up to light ring** (or photon orbit) and then …

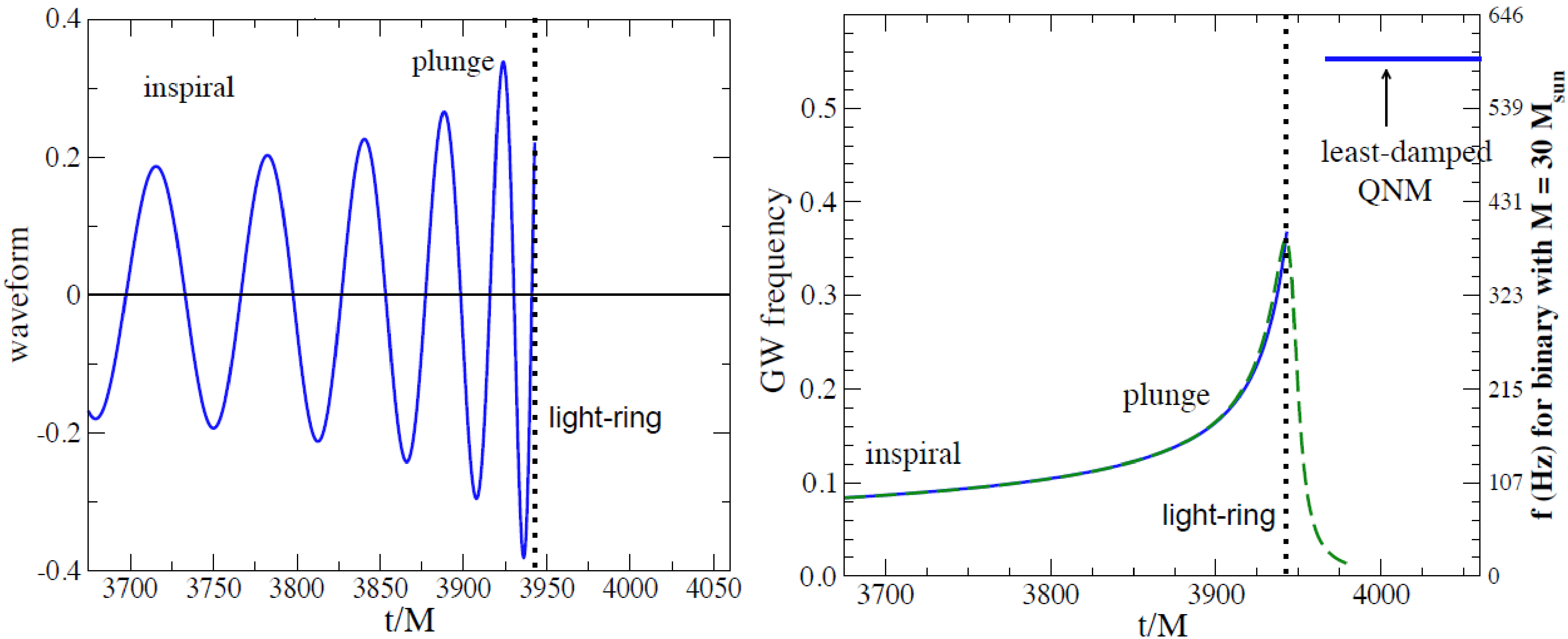

- **Quasi-normal modes** excited at **light-ring crossing**

(Goebel 1972, Davis et al. 1972, Ferrari et al. 1984, Damour et al. 07, Barausse et al. 11, Price et al. 15)

EFFECTIVE-ONE-BODY WAVEFORMS

… attach **superposition** of **quasi-normal modes** of **remnant** black hole.

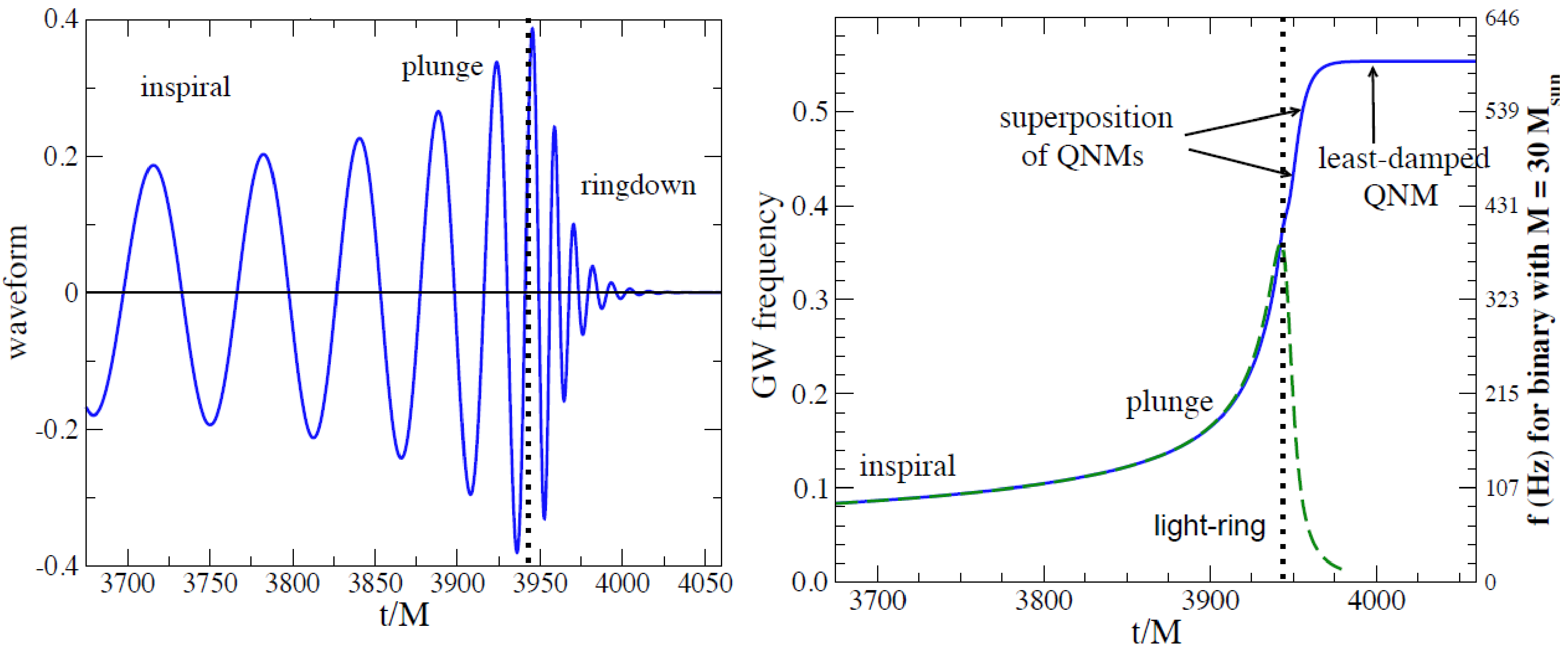

$$h_{22}^{\rm IMR}(t) = h_{22}^{\rm insp-plunge}\,\theta(t_{\rm match}-t) + h_{22}^{\rm merger-RD}\theta(t-t_{\rm match})$$

$$h_{22}^{\rm merger-RD}(t) = \sum_{n=0}^{N-1} A_n\, e^{-i\sigma_{22n}(t-t_{\rm match})} \qquad \sigma_{22n} \equiv \omega_{22n} - i/\tau_{22n}$$

GW150914 QUASI-NORMAL MODES

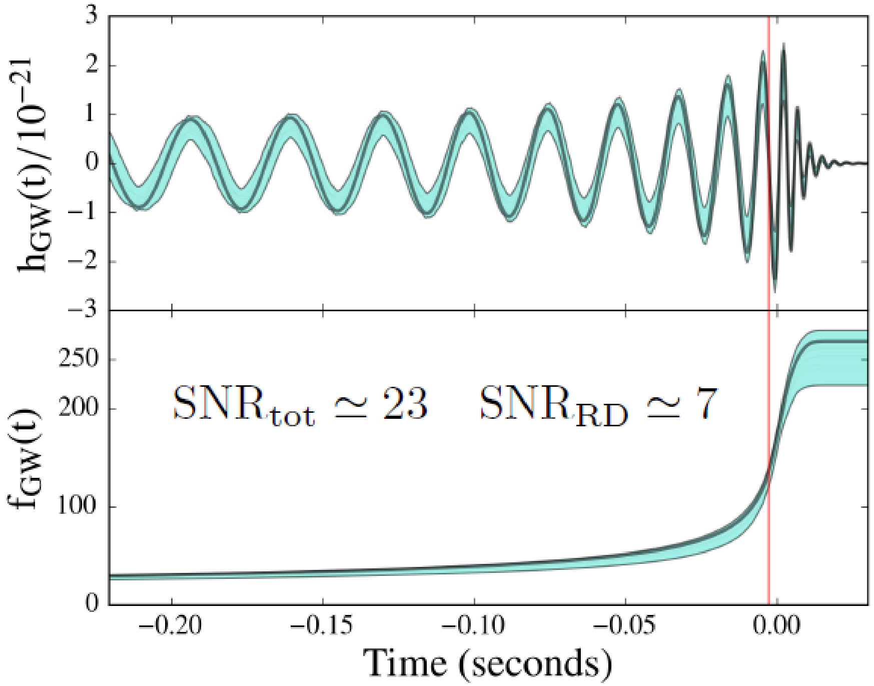

(Abbott et al. PRL 116 (2016) 221101)

- Bayesian analysis with **damped-sinusoid template** to extract **frequency** and **decay time**, **starting at different times** after merger.

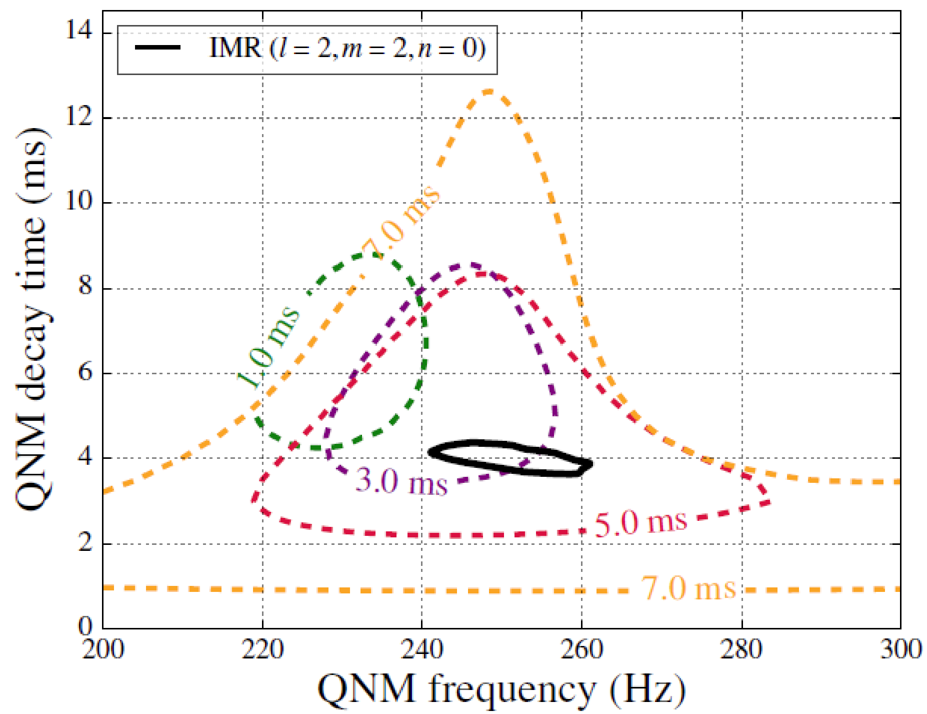

- Starting **from 5 msec** after merger, posterior distributions of **frequencies** and **decay times** from **damped sinusoid** and **IMR waveform** are **consistent**.
- First (low-accuracy) verification of **black hole uniqueness** properties (?)

ECHOES FROM THE ABYSS?

For a GR-BH the excitation of observable spacetime modes happens at the photon sphere (r_p ~ 3M)
The vibrations travel otward to observers and inward to the horizon (r_g = 2M) where it dies off

For a compact object with an effective surface at r_s = 2M (1+ε), at later times the pulse traveling inwards is reflected at its surface. Upon each interaction, a fraction exits to outside observers, giving rise to a series of echoes

The appearance of late-time echoes in the waveform (due to waves trapped into the photon sphere-surface cavity) would be a smoking-gun for new physics

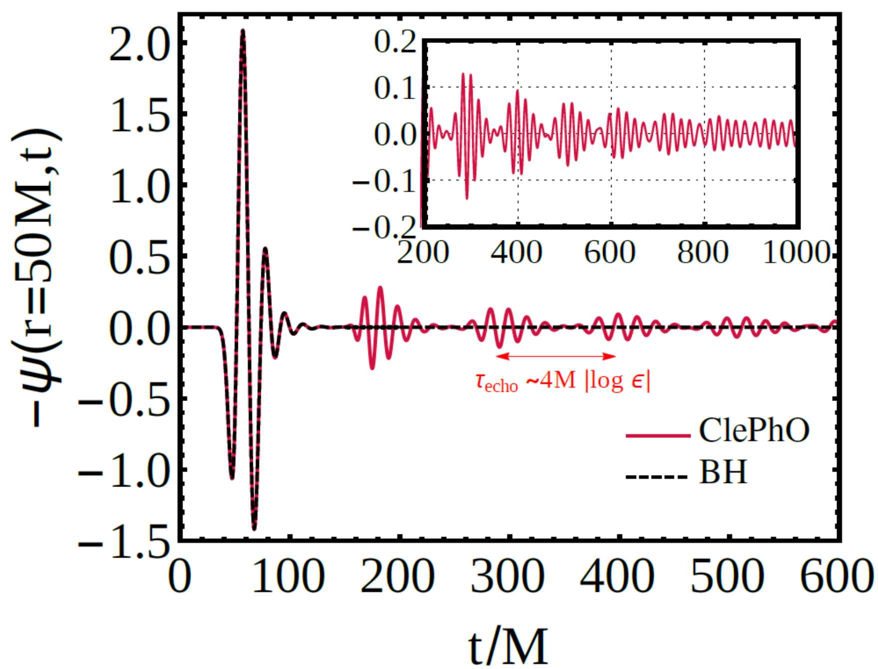

arXiv:1707.03021

PARAMETRISED TESTS OF GR

- GW waveforms are expressed in terms of effective series, for the Phenom family:

$$h(f;\theta) = A(f;\theta)e^{i\Phi(f;\theta)}$$

$$\Phi(f;\theta) = \sum_{k=0}^{7}(\varphi_k + \varphi_k^{(l)})f^{(k-5)/3} + \sum_{i\neq k}\varphi_i g(f)$$

post-Newtonian series   effective series

$$\varphi_j \equiv \varphi_j(m_1, m_2, \vec{s}_1, \vec{s}_2)$$

- Modified theories of gravity change the series (e.g. PPE: Yunes & Pretorius, arXiv:0909.3328, Cornish+,arXiv: 1105.2088)

- Perturb the GW phase around GR (Li+,arXiv:1110.0530, Agathos+,arXiv:1311.0420)

$$\hat{\varphi}_j \equiv \varphi_j^{GR}(1+\delta\hat{\varphi}_j) \qquad \delta\hat{\varphi}_j = 0 \iff \text{GR}$$

- Bound violations by computing posterior distributions for the $\delta\hat{\varphi}_j$ in concert with the physical parameters of the system

waveform regime	parameter	f−dependence	
early-inspiral regime	$\delta\hat{\varphi}_0$	$f^{-5/3}$	post-Newtonian
	$\delta\hat{\varphi}_1$	$f^{-4/3}$	
	$\delta\hat{\varphi}_2$	f^{-1}	
	$\delta\hat{\varphi}_3$	$f^{-2/3}$	
	$\delta\hat{\varphi}_4$	$f^{-1/3}$	
	$\delta\hat{\varphi}_{5l}$	$\log(f)$	
	$\delta\hat{\varphi}_6$	$f^{1/3}$	
	$\delta\hat{\varphi}_{6l}$	$f^{1/3}\log(f)$	
	$\delta\hat{\varphi}_7$	$f^{2/3}$	
intermediate regime	$\delta\hat{\beta}_2$	$\log f$	effective
	$\delta\hat{\beta}_3$	f^{-3}	
merger–ringdown regime	$\delta\hat{\alpha}_2$	f^{-1}	
	$\delta\hat{\alpha}_3$	$f^{3/4}$	
	$\delta\hat{\alpha}_4$	$\tan^{-1}(af+b)$	

LVC, arXiv:1602.03841

CURRENT CONSTRAINTS

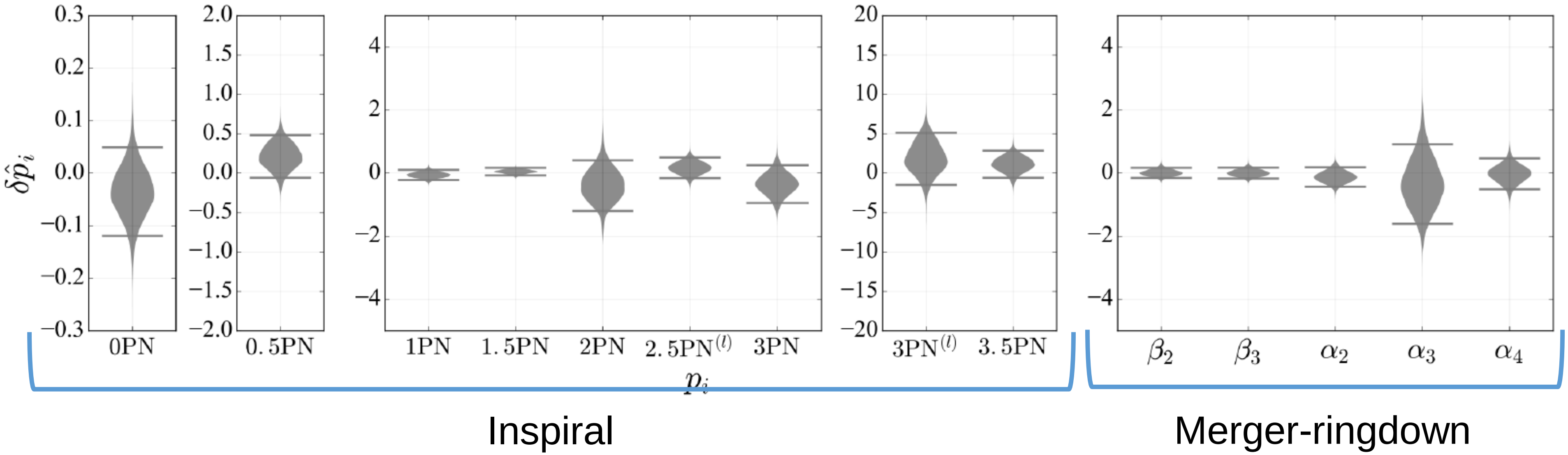

Posterior distributions for $\delta\varphi_j$ show no evidence for violations of GR

PROPAGATION TESTS: MASSIVE GRAVITY

- Families of alternative theories modify the propagation of GW
- Massive gravity (e.g. Will, arXiv:9709011)

$$E^2 = p^2 v_g^2 + m_g^2 c^4$$

$$v_g^2/c^2 \simeq 1 - \frac{h^2 c^2}{\lambda_g^2 E^2} \qquad \lambda_g = \frac{h}{m_g c}$$

- GW phase affected

$$\Delta\Phi = -\frac{\pi^2 D M}{\lambda_g^2 (1+z)}$$

- GW constrains gravitons Compton wavelength

$$m_g \leq 1.2 \times 10^{-22} \mathrm{eV/c^2}\ (90\%)$$

$$\lambda_g \geq 10^{13} \mathrm{km}\ (90\%)$$

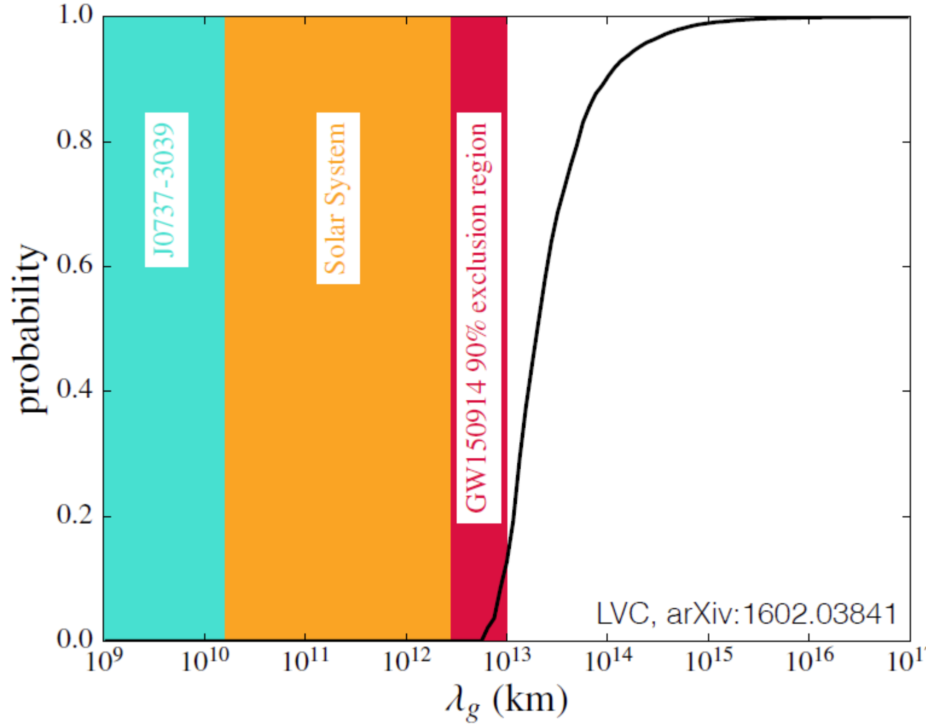

Current constraint, LVC, arXiv:1706.01812

$$\lambda_g > 1.6 \times 10^{13}\ \mathrm{km}$$

$$m_g \leq 7.7 \times 10^{-23}\ \mathrm{eV}/c^2$$

GW POLARISATION

- Gravitational waves in general relativity are transverse, tensorial waves
- Extensions to general relativity predict up to six polarisation states
    - Two transverse tensor states
    - Two longitudinal vector states
    - Two scalar states, one longitudinal and one "breathing"

Theory	+	x	x	y	b	l
General Relativity	allowed	allowed	forbidden	forbidden	forbidden	forbidden
GR in noncompactified 4/6D Minkowski	allowed	allowed	allowed	allowed	allowed	allowed
Einstein-Æther	allowed	allowed	allowed	allowed	allowed	allowed
5D Kaluza-Klein	allowed	allowed	allowed	allowed	allowed	forbidden
Randall-Sundrum braneworld	allowed	allowed	forbidden	forbidden	forbidden	forbidden
Dvali-Gabadadze-Porrati braneworld	allowed	allowed	depends	depends	depends	depends
Brans-Dicke	allowed	allowed	forbidden	forbidden	allowed	allowed
f(R) gravity	allowed	allowed	forbidden	forbidden	allowed	allowed
Bimetric theory	allowed	allowed	allowed	allowed	allowed	allowed
Four-Vector Gravity	forbidden	forbidden	allowed	allowed	forbidden	forbidden

Nishizawa et al., Phys. Rev. D 79, 082002 (2009) [except G4v & Einstein-Æther]. allowed / depends / forbidden

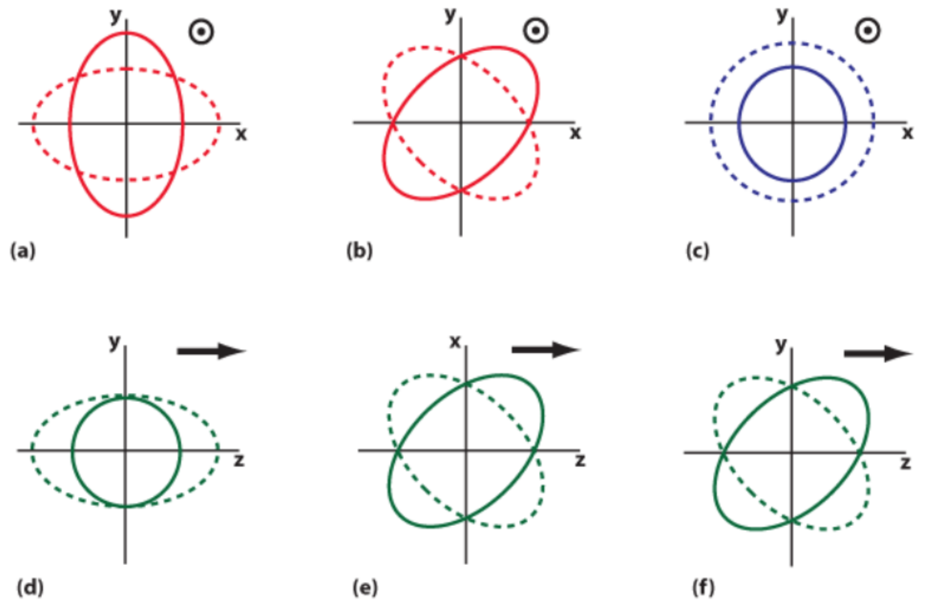

DETECTOR RESPONSE

- Each polarisation state couples to the detector differently $h = \sum_{k=1}^{6} F_k h_k$

Antenna response functions F_k

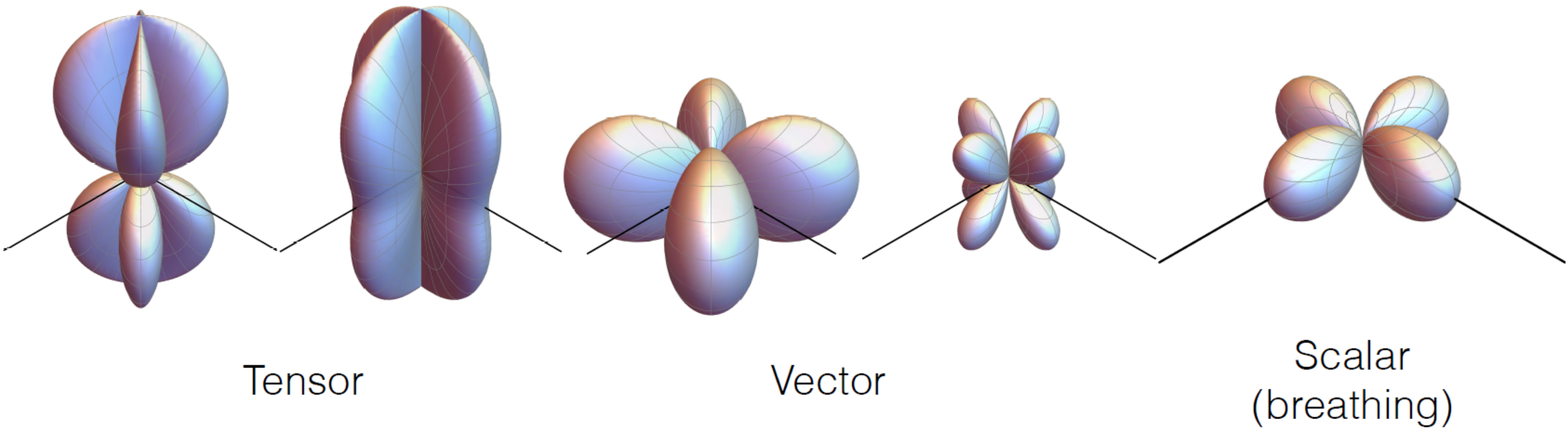

- In principle detectable with more than one detector

Courtesy of Max Isi

- The two LIGO detectors could not discriminate among different polarisation states (essentially aligned)
- A third detector is necessary

GW170814: POLARISATION

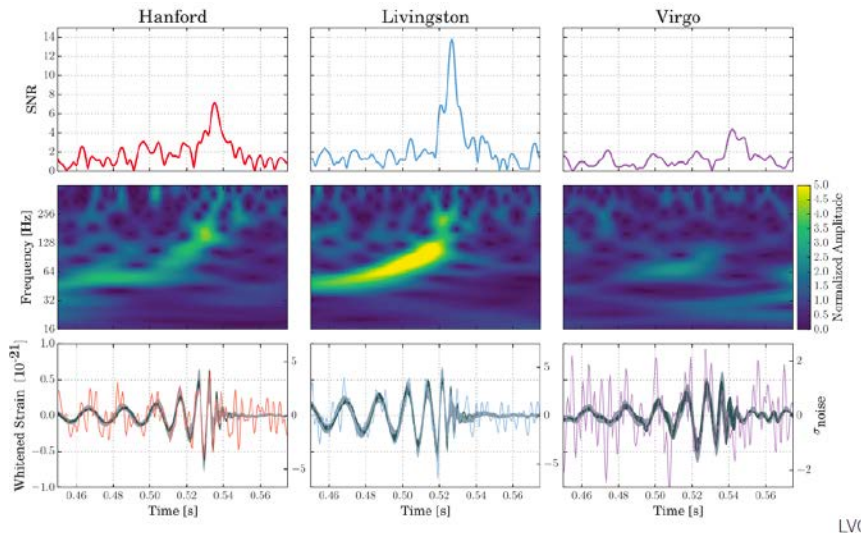

- Virgo improves dramatically the position reconstruction
- Break degeneracy with polarisation states
- Evidence for pure tensor GW against pure scalar (or pure vector)

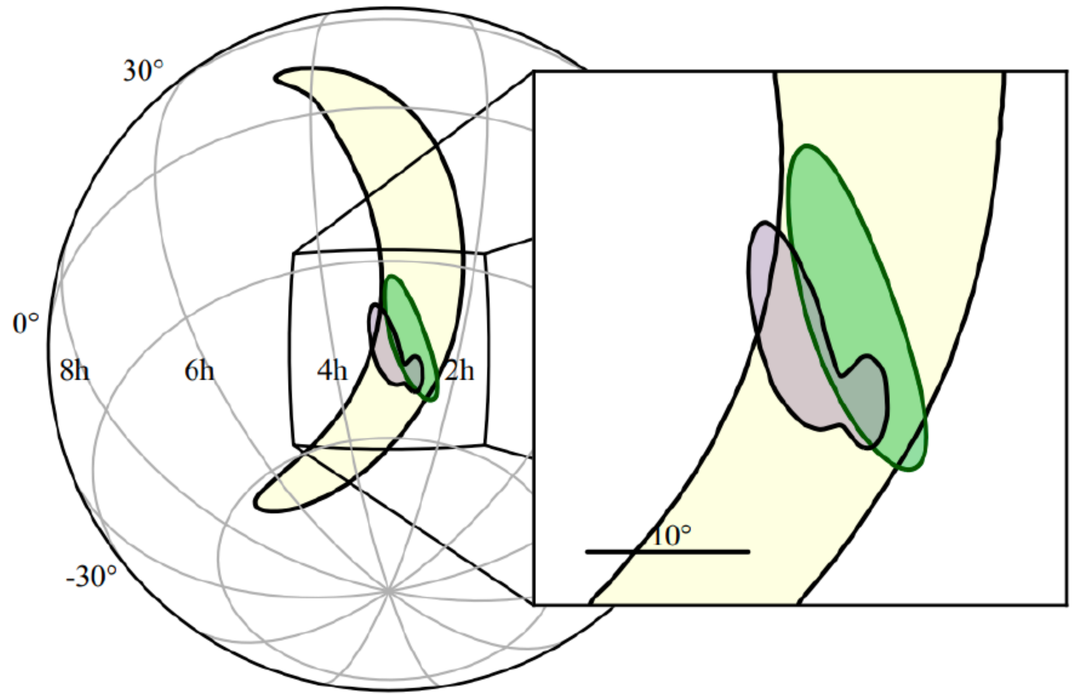

LIGO-VIRGO BLACK HOLES

All the current observational evidence gathered around massive, compact and dark objects is compatible with the GR-BH hypothesis (two-parameter Kerr geometry)

Despite this, there are long-standing problems associated with horizons and singularities, which hint at some inconsistency between classical gravity and quantum mechanics at the scale of the horizon that could be tested (echoes, qnm spectrum, tidal deformability)

GW event	Detection time (UTC)	Date published	Location area[n 1] (deg^2)	Luminosity distance (Mpc)[n 2]	Energy radiated ($c^2 M_\odot$)[n 3]	Chirp mass ($M_\odot$)[n 4]	Primary		Secondary		Remnant		
							Type	Mass ($M_\odot$)	Type	Mass ($M_\odot$)	Type	Mass ($M_\odot$)	Spin[n 5]
GW150914	2015-09-14 09:50:45	2016-02-11	600; mostly to the south	440^{+160}_{-180}	$3.0^{+0.5}_{-0.5}$	$28.2^{+1.8}_{-1.7}$	BH[n 6]	$35.4^{+5.0}_{-3.4}$	BH[n 7]	$29.8^{+3.3}_{-4.3}$	BH	$62.2^{+3.7}_{-3.4}$	$0.68^{+0.05}_{-0.06}$
LVT151012 (fr)	2015-10-12 09:54:43	2016-06-15	1600	1000^{+500}_{-500}	$1.5^{+0.3}_{-0.4}$	$15.1^{+1.4}_{-1.1}$	BH	23^{+18}_{-6}	BH	13^{+4}_{-5}	BH	35^{+14}_{-4}	$0.66^{+0.09}_{-0.10}$
GW151226	2015-12-26 03:38:53	2016-06-15	850	440^{+180}_{-190}	$1.0^{+0.1}_{-0.2}$	$8.9^{+0.3}_{-0.3}$	BH	$14.2^{+8.3}_{-3.7}$	BH	$7.5^{+2.3}_{-2.3}$	BH	$20.8^{+6.1}_{-1.7}$	$0.74^{+0.06}_{-0.06}$
GW170104	2017-01-04 10:11:58	2017-06-01	1200	880^{+450}_{-390}	$2.0^{+0.6}_{-0.7}$	$21.1^{+2.4}_{-2.7}$	BH	$31.2^{+8.4}_{-6.0}$	BH	$19.4^{+5.3}_{-5.9}$	BH	$48.7^{+5.7}_{-4.6}$	$0.64^{+0.09}_{-0.20}$
GW170608	2017-06-08 02:01:16	2017-11-16	520; to the north	340^{+140}_{-140}	$0.85^{+0.07}_{-0.17}$	$7.9^{+0.2}_{-0.2}$	BH	12^{+7}_{-2}	BH	7^{+2}_{-2}	BH	$18.0^{+4.8}_{-0.9}$	$0.69^{+0.04}_{-0.05}$
GW170814	2017-08-14 10:30:43	2017-09-27	60; towards Eridanus	540^{+130}_{-210}	$2.7^{+0.4}_{-0.3}$	$24.1^{+1.4}_{-1.1}$	BH	$30.5^{+5.7}_{-3.0}$	BH	$25.3^{+2.8}_{-4.2}$	BH	$53.2^{+3.2}_{-2.5}$	$0.70^{+0.07}_{-0.05}$

GW170817: A BINARY NEUTRON STAR MERGER

Combined SNR = 32.4
- LIGO-Livingston: 26.4
- LIGO-Hanford: 18.8
- Virgo: 2.0

GW170817 swept through the detectors' sensitive band in ~100 s (f_{start} = 24 Hz)
~3000 cycles in band

Initial sky localization ~28 deg^2

Identified by matched filtering the data against post-Newtonian waveform models

Virgo data used for sky localization and estimation of the source properties

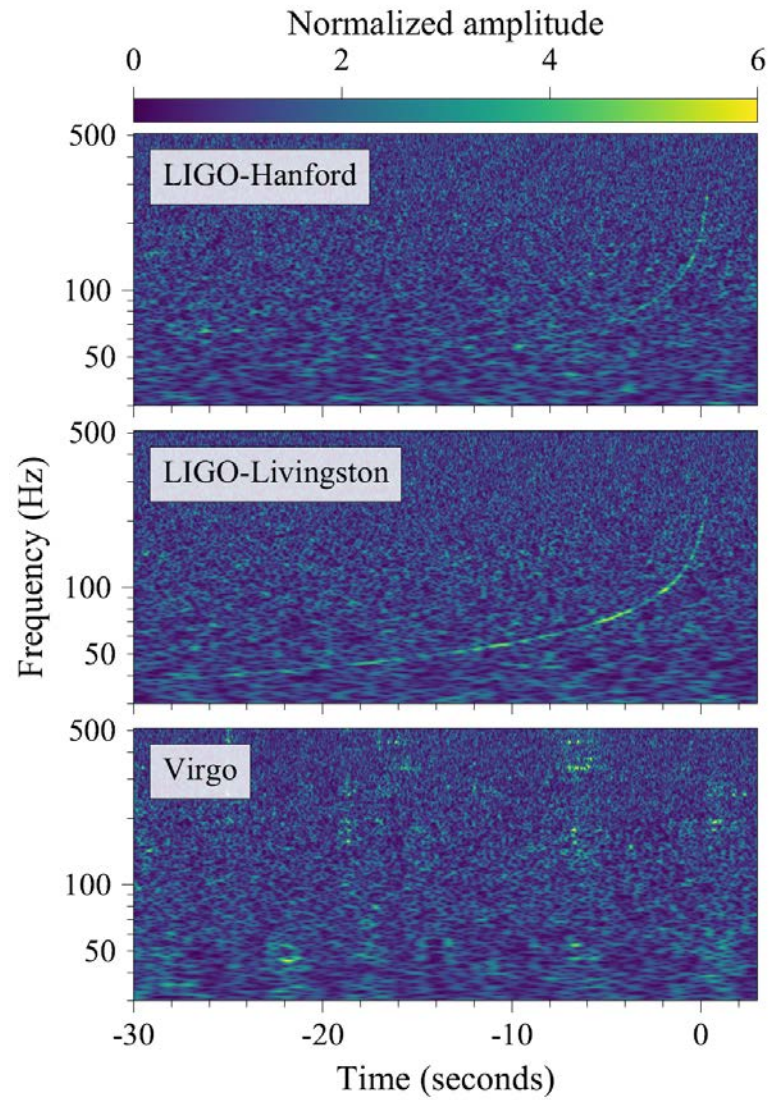

PRL 119, 161101 (2017)

TIDAL EFFECTS

Leading-order tidal effect in the post-Newtonian waveform phase depends on two dimensionless Love numbers (which can potentially take large values) :

$$\hat{\lambda}_i = \frac{\lambda_i}{m_i^5} = \frac{2}{3} k_2(\mathrm{EOS}, m_i) \left(\frac{R_i}{m_i}\right)^5$$

$$\hat{\lambda}_i(1.4 M_\odot) \approx 65\text{–}1600$$

$$\hat{\lambda}_i(1.35 M_\odot) \approx 140\text{–}2300$$

$$\hat{\lambda}_i(1.2 M_\odot) \approx 400\text{–}4400$$

$$\varphi(f) = \varphi_0 - \frac{1}{32\eta v^5}\Big\{1 + v^2 c_{1\mathrm{PN}}(\eta) + v^3 c_{1.5\mathrm{PN}}(\eta, \chi_{\mathrm{eff}}) \cdots + c_{4\mathrm{PN}} v^8 + c_{4.5\mathrm{PN}} v^9$$
$$+ v^{10}\left\{c_{5\mathrm{PN}} + 3\left[(1 + 7\eta - 31\eta^2)(\hat{\lambda}_1 + \hat{\lambda}_2) - \sqrt{1-4\eta}(1 + 9\eta - 11\eta^2)(\hat{\lambda}_1 - \hat{\lambda}_2)\right]\right\} + c_{5.5\mathrm{PN}} v^{11}$$
$$+ v^{12}\Big\{c_{6\mathrm{PN}} + \frac{585}{56}\Big[\left(1 + \frac{3775}{234}\eta - \frac{389}{6}\eta^2 + \frac{1376}{117}\eta^3\right)(\hat{\lambda}_1 + \hat{\lambda}_2)$$
$$-\sqrt{1-4\eta}\left(1 + \frac{4243}{234}\eta - \frac{6217}{234}\eta^2 - \frac{10}{9}\eta^3\right)(\hat{\lambda}_1 - \hat{\lambda}_2)\Big]\Big\}\Big\}$$

Only certain combinations of Love numbers enter the waveform: [MF PRL'14]

$$\tilde{\Lambda}(\eta, \hat{\lambda}_1, \hat{\lambda}_2), \delta\tilde{\Lambda}(\eta, \hat{\lambda}_1, \hat{\lambda}_2)$$

$$\varphi(f) = \varphi_0 - \frac{1}{32\eta v^5}\Big\{1 + v^2 c_{1\mathrm{PN}}(\eta) + v^3 c_{1.5\mathrm{PN}}(\eta, \chi_{\mathrm{eff}}) \cdots + c_{4\mathrm{PN}} v^8 + c_{4.5\mathrm{PN}} v^9$$
$$+ v^{10}\left\{c_{5\mathrm{PN}} + \frac{39}{8}\tilde{\Lambda}\right\} + c_{5.5\mathrm{PN}} v^{11} + v^{12}\left\{c_{6\mathrm{PN}} + \frac{3115}{128}\tilde{\Lambda} - \frac{6595}{728}\delta\tilde{\Lambda}\right\}\Big\}$$

For equal masses:

$$\tilde{\Lambda} = \hat{\lambda}_1 = \hat{\lambda}_2, \delta\tilde{\Lambda} = 0$$

For unequal masses:

$$\delta\tilde{\Lambda} \lesssim 0.01\tilde{\Lambda}$$

Only $\tilde{\Lambda}$ measureable.

Further, non-tidal 4PN terms and higher are unknown; leads to systematic errors. [MF PRL'14]

PROBING THE STRUCTURE OF NEUTRON STARS

Tidal deformability give support for “soft” EOS, leading to more compact NS. Various models can now be excluded. We can place the additional constraint that the EOS must support a NS with $1.97\,\mathrm{M}_\odot$

Leading tidal contribution to GW phase appears at 5 PN: $\tilde{\Lambda} = \frac{16}{13}\frac{(m_1 + 12m_2)m_1^4\Lambda_1 + (m_2 + 12m_1)m_2^4\Lambda_2}{(m_1 + m_2)^5}$

Employ common EOS for both NS (green shading), EOS insensitive relations (green), parametrized EOS (blue), independent EOSs (orange)

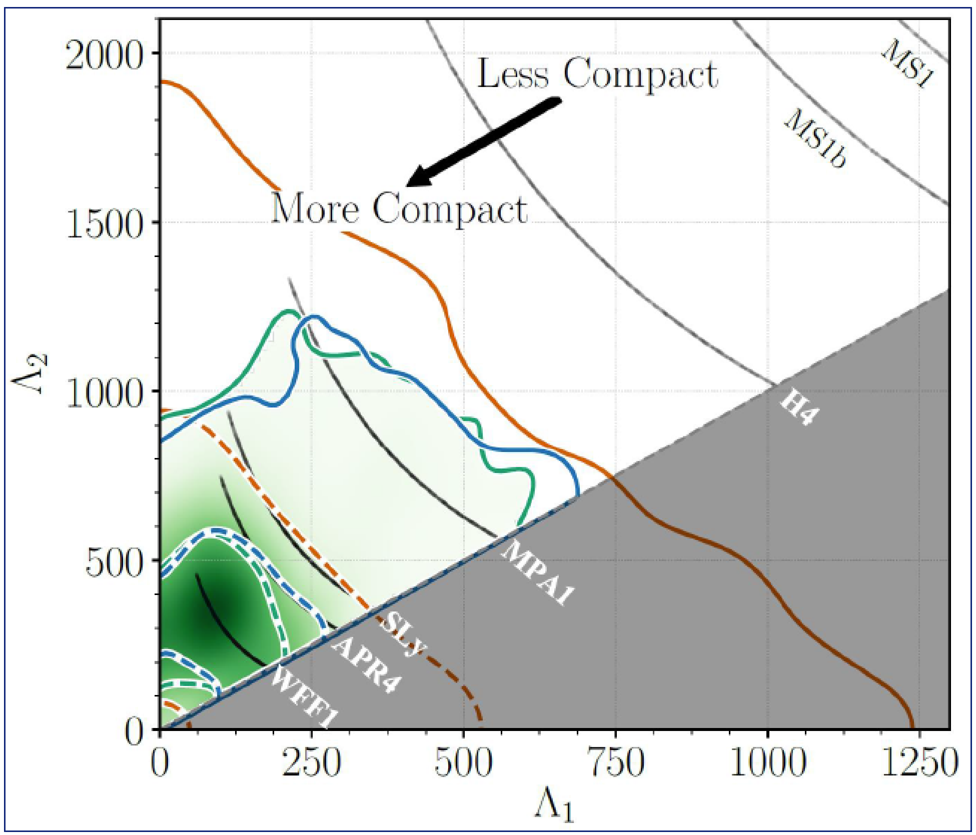

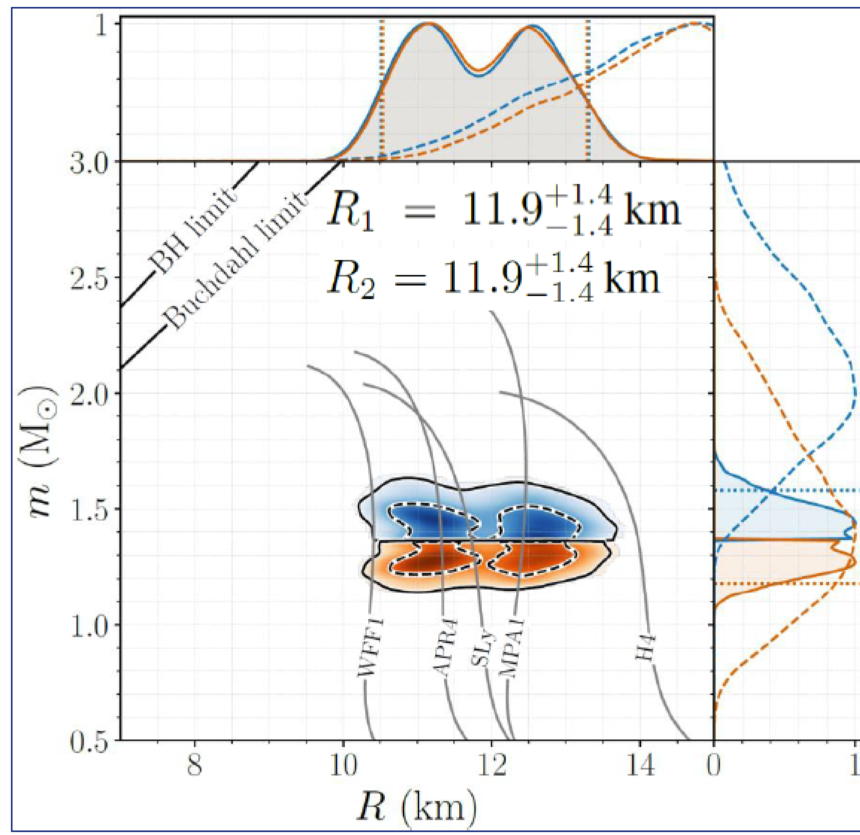

GRB 170817A

The Fermi Gamma-ray Burst Monitor Independently detected a gamma-ray burst (GRB170817A) with a time-delay of
1.734 ± 0.054 s with respect to the merger time

The probability of a chance temporal and spatial association of GW170817 and GRB 170817A is
5.0×10^{-8}

Binary neutron star (BNS) mergers are progenitors of (at least some) SGRBs

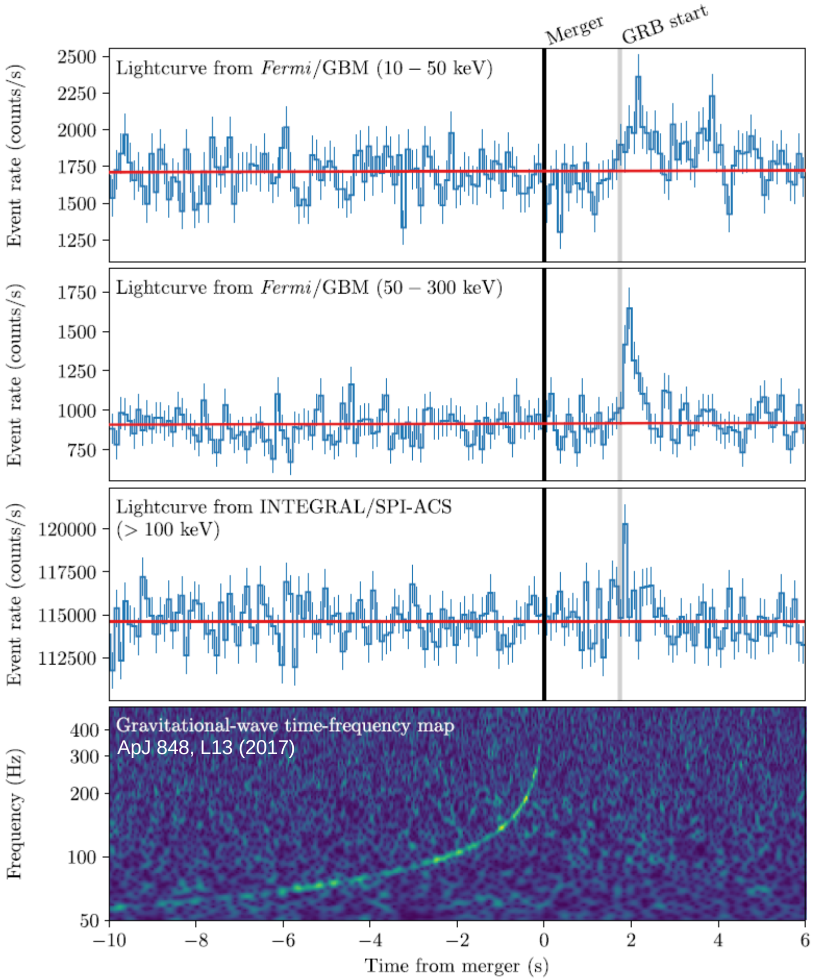

Astrophys. J. Lett. 848, L13 (2017)

IMPLICATIONS FOR FUNDAMENTAL PHYSICS

Gamma rays reached Earth 1.7 s after the end of the gravitational wave inspiral signal. The data are consistent with standard EM theory minimally coupled to general relativity

GWs and light propagation speeds

Identical speeds to about 1 part in 10^{15}

Test of Equivalence Principle

According to General Relativity, GW and EM waves are deflected and delayed by the curvature of spacetime produced by any mass (i.e. background gravitational potential). Shapiro delays affect both waves in the same manner

$$\delta t_{\rm S} = -\frac{1+\gamma}{c^3}\int_{\mathbf{r}_e}^{\mathbf{r}_o} U(\mathbf{r}(l))dl.$$

Milky Way potential gives same effect to within about 1 part in a million

$$-1.2 \times 10^{-6} \leq \gamma_{\rm GW} - \gamma_{\rm EM} \leq 2.6 \times 10^{-7}$$

Including data on peculiar velocities to 50 Mpc: gives the same effect to within 4 parts in a billion

$$\Delta\gamma \leq 4 \times 10^{-9}.$$

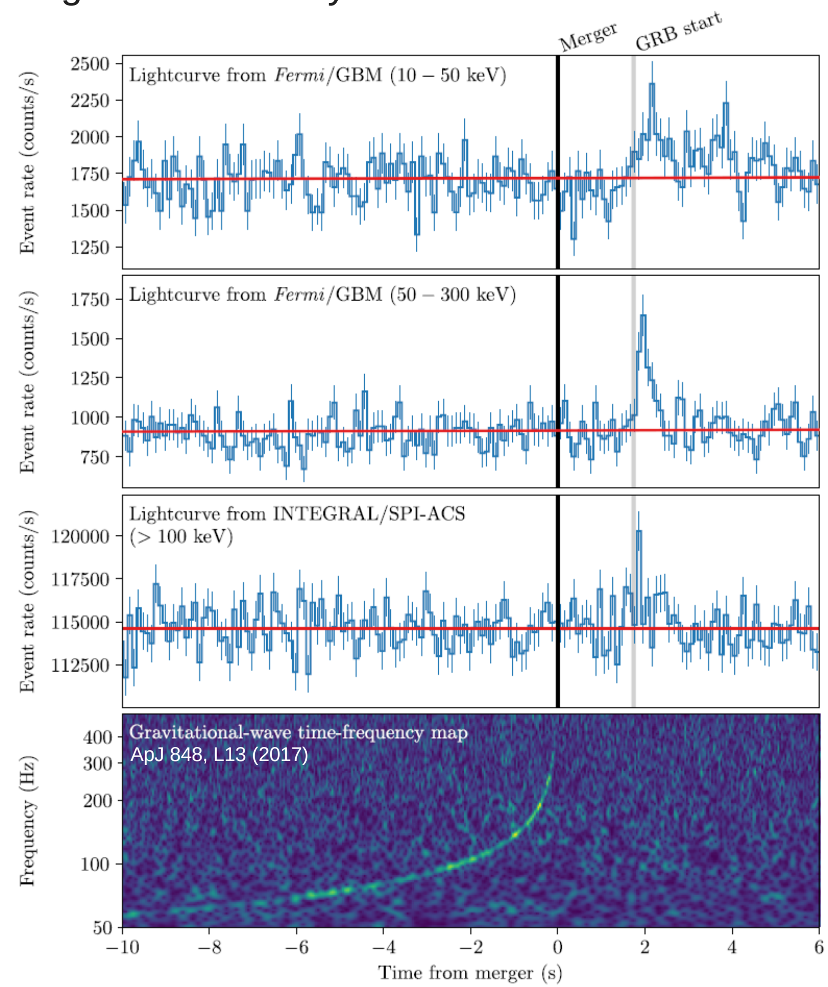

DARK ENERGY AND DARK MATTER AFTER GW170817

GW170817 had consequences for our understanding of Dark Energy and Dark Matter

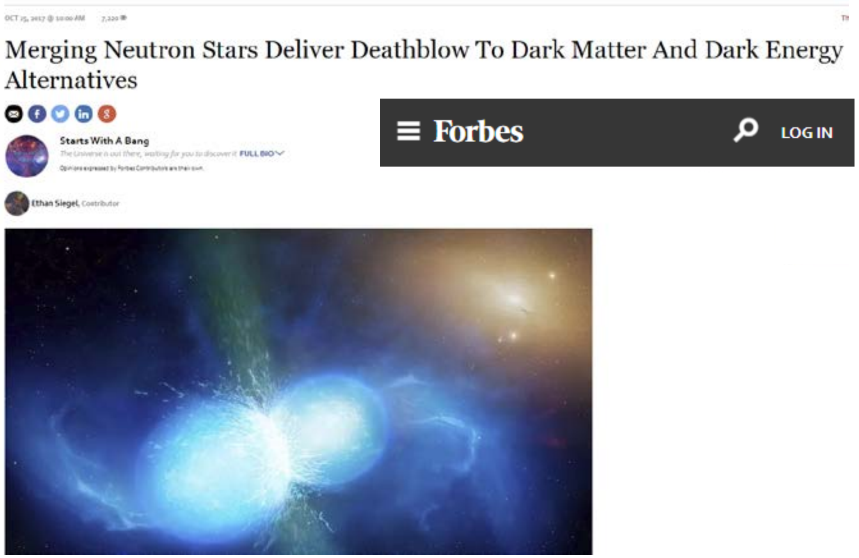

GW170817 falsifies Dark Matter Emulators

No-dark-matter modified gravity theories like TeVeS or MoG/Scalar-Tensor-Vector ideas have the property that GW propagate on different geodesics (normal matter) from those followed by photons and neutrinos (effective mass to emulate dark matter)

This would give a difference in arrival times between photons and gravitational waves by approximately 800 days, instead of the 1.7 seconds observed

arXiv:1710.06168

Dark Energy after GW170817

Adding a scalar field to a tensor theory of gravity, yields two generic effects:

1. There's generally a *tensor speed excess* term, which modifies (increases) the propagation speed of GW
2. The scale of the effective Planck mass changes over cosmic times, which alters the damping of the gravitational wave signal as the Universe expands

Simultaneous detection of GW and EM signals rules out a class of modified gravity theories

A large class of scalar-tensor theories and DE models are highly disfavored, e.g. covariant Galileon, but also other gravity theories predicting varying cg such as Einstein-Aether, Horava gravity, Generalized Proca, TeVeS and other MOND-like gravities

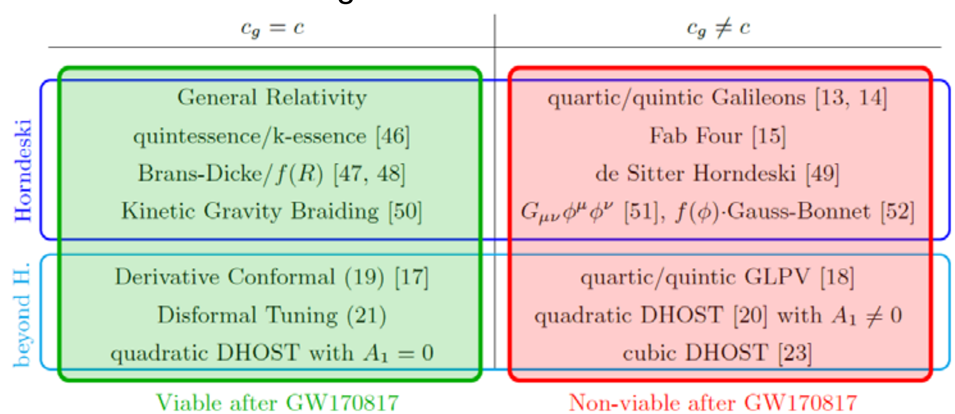

PRL 119, 251304 (2017)

LOCALIZATION

Improved localization of GW170817, with the location of the associated counterpart SSS17a/AT 2017gfo has been obtained. The darker and lighter blue shaded regions correspond to 50% and 90% credible regions respectively, and the gray shaded region shows the previously derived 90% credible region presented in B. Abbott et al., PRL **119**, 161101 (2017)

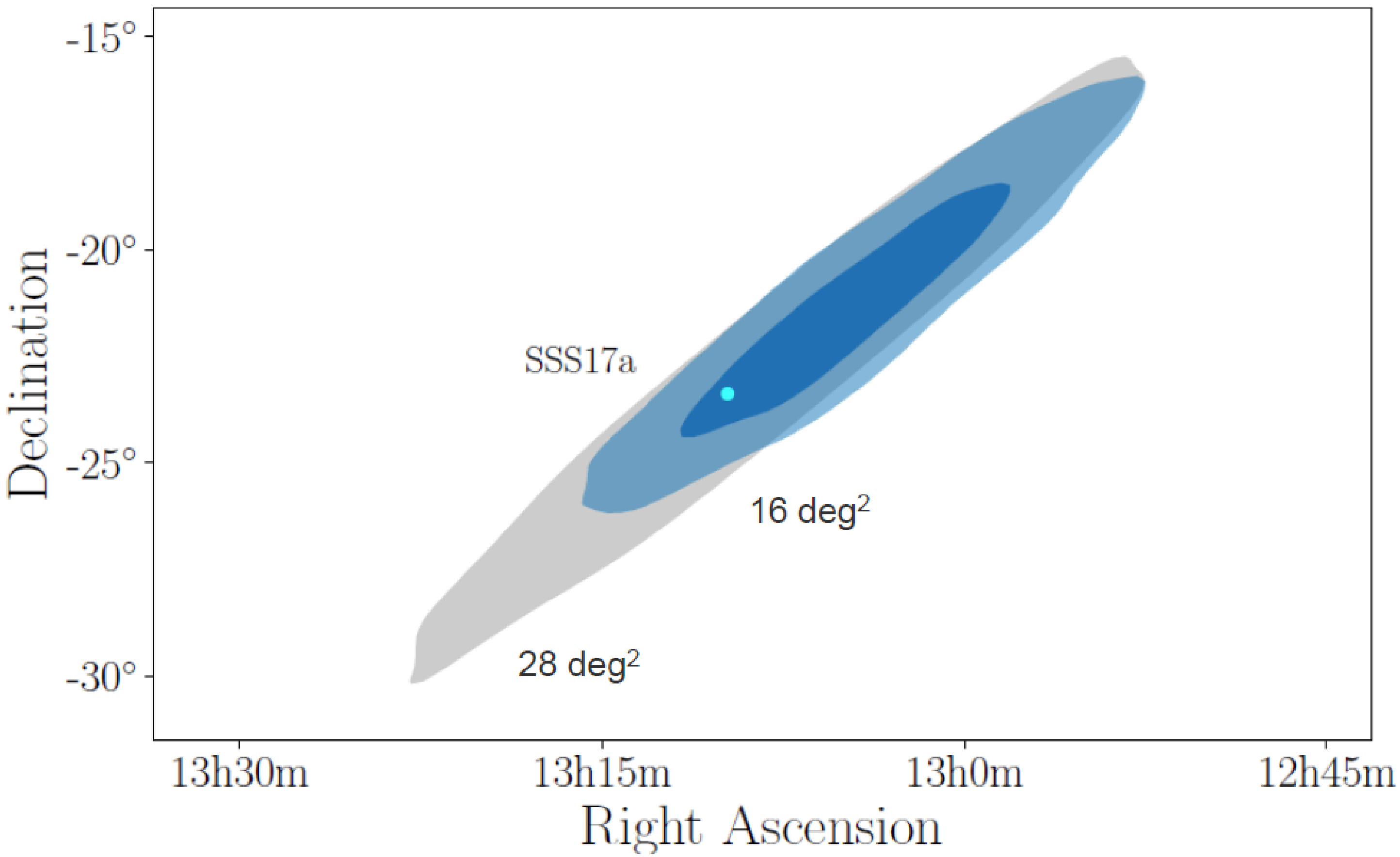

Despite low SNR, Virgo was essential to improved localization and EM follow-up.

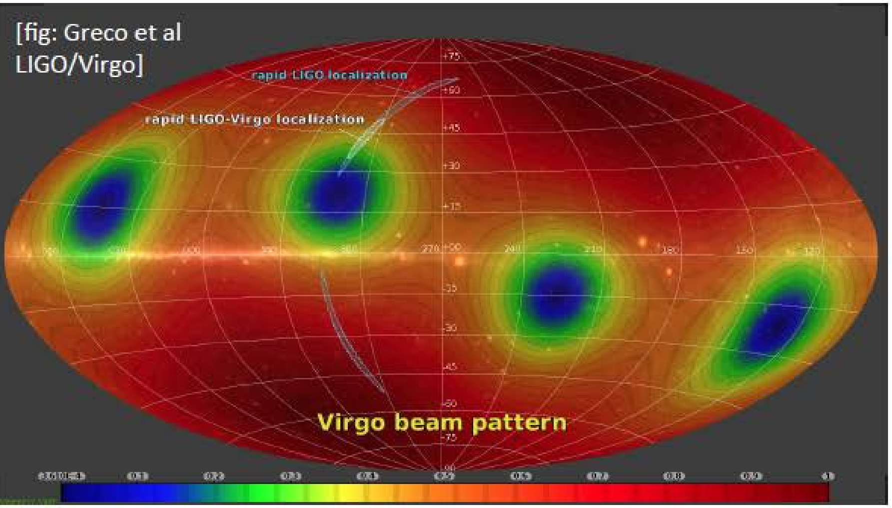

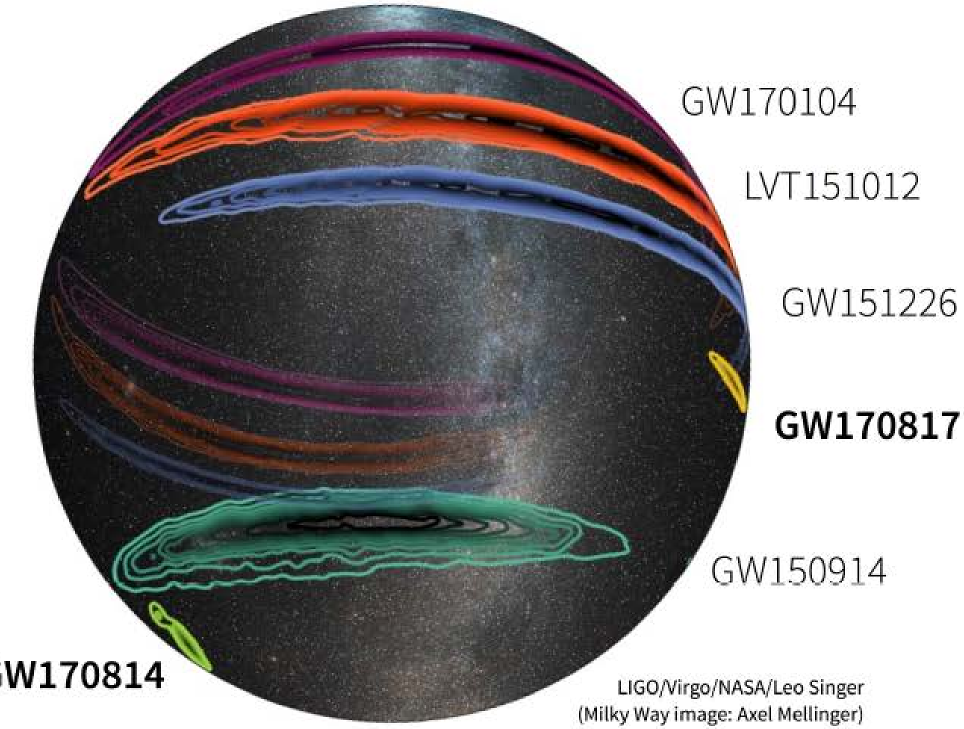

Source	SNR	$\Delta\Omega$ (sq. deg.)	d_L (Mpc, median)
GW150914	23.7	230	420
LVT151012	9.7	1600	1000
GW151226	12.0	850	440
GW170104	13.0	1200	880
GW170608	13	520	340
GW170814	18.3	60	540
(HLV)=(9.7, 14.8, 4.8)			
GW170817	32.4	28	40
(HLV)=(18.8, 26.4, 2.0)			

(median values from LSC papers, dropping error bars)

GW170817: START OF MULTIMESSENGER ASTRONOMY

GW170817 was observed by about 70 observatories all over Earth (including Antarctica) and in space

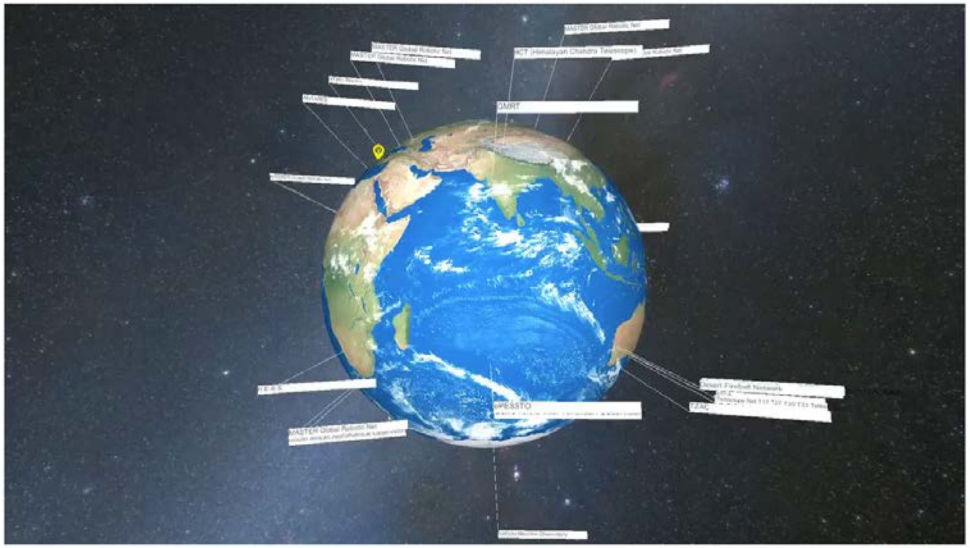

Astrophys. J. Lett. 848, L12 (2017)

Location of the apparent host galaxy **NGC 4993** in the Swope optical discovery image
10.9 hrs after the merger

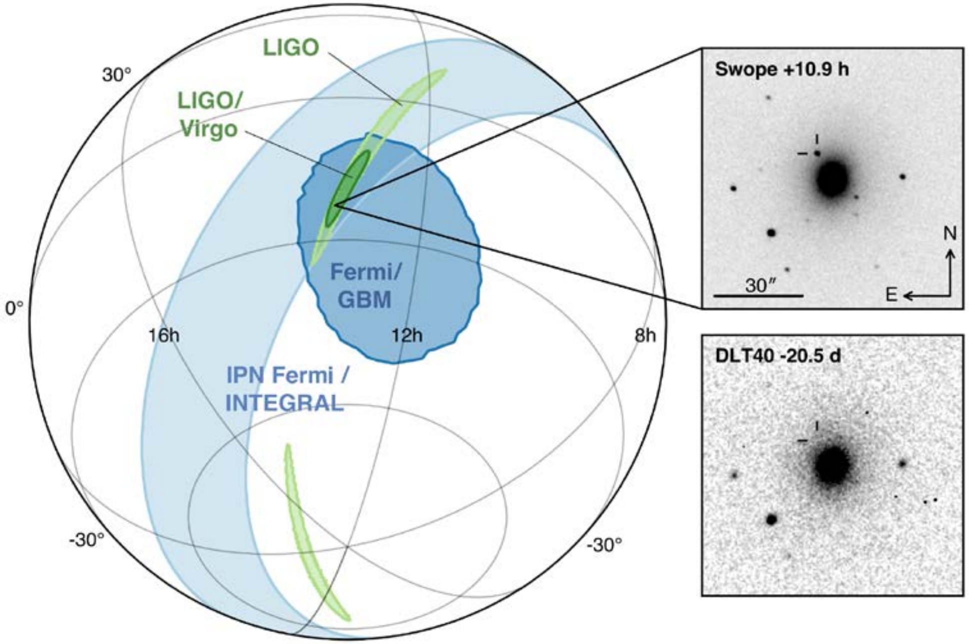

A NEW STANDARD CANDLE

A few tens of detections of binary neutron star mergers allow determining the Hubble parameters to about 1% accuracy

Measurement of the local expansion of the Universe

The Hubble constant

- Distance from GW signal
- Redshift from EM counterpart (galaxy NGC 4993)

LVC, Nature 551, 85 (2017)

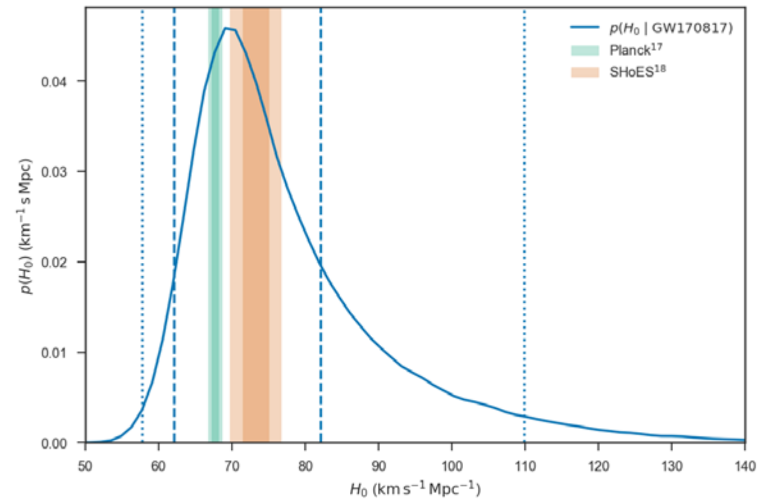

GW170817

- One detection: limited accuracy
- Few tens of detections with LIGO/Virgo will be needed to obtain O(1%) accuracy

Del Pozzo, PRD 86, 043011 (2012)

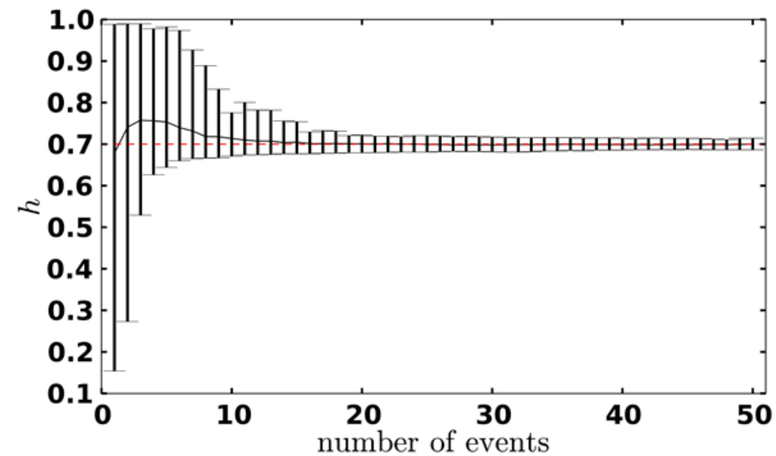

Third generation observatories allow studies of the Dark Energy equation of state parameter

FROM O2 TO O3

Short term plans and activity

FROM O2 TO O3

← 12 months →

O2

Comm.

Upgrades

- Monolithic suspension re-installation
- Vacuum upgrade for dust protection
- AEI squeezer
- High power laser
- Newtonian noise sensors test installation

Comm.

O3

Strategy:

- Reserve commissioning time
- Limit the number of upgrades

Target sensitivity for O3: 60 Mpc

- Main benefit should come from putting back the monolithic suspension
  - Removing the steel wire thermal noise from noise budget gives a 20 Mpc range increase
- Theoretical limits: 100 Mpc @13W, no squeezing

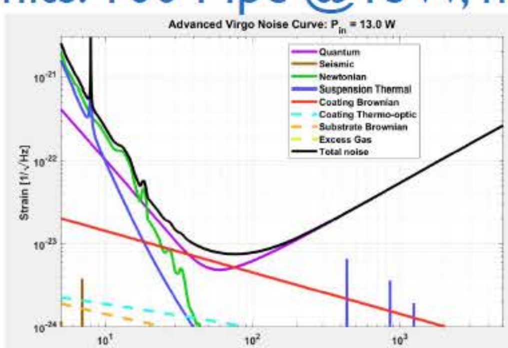

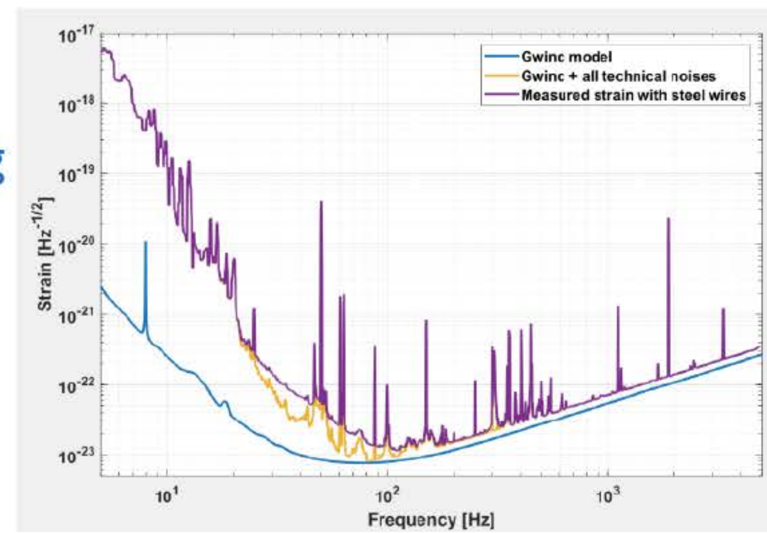

CREDIT: B. Mours

FROM O2 TO O3

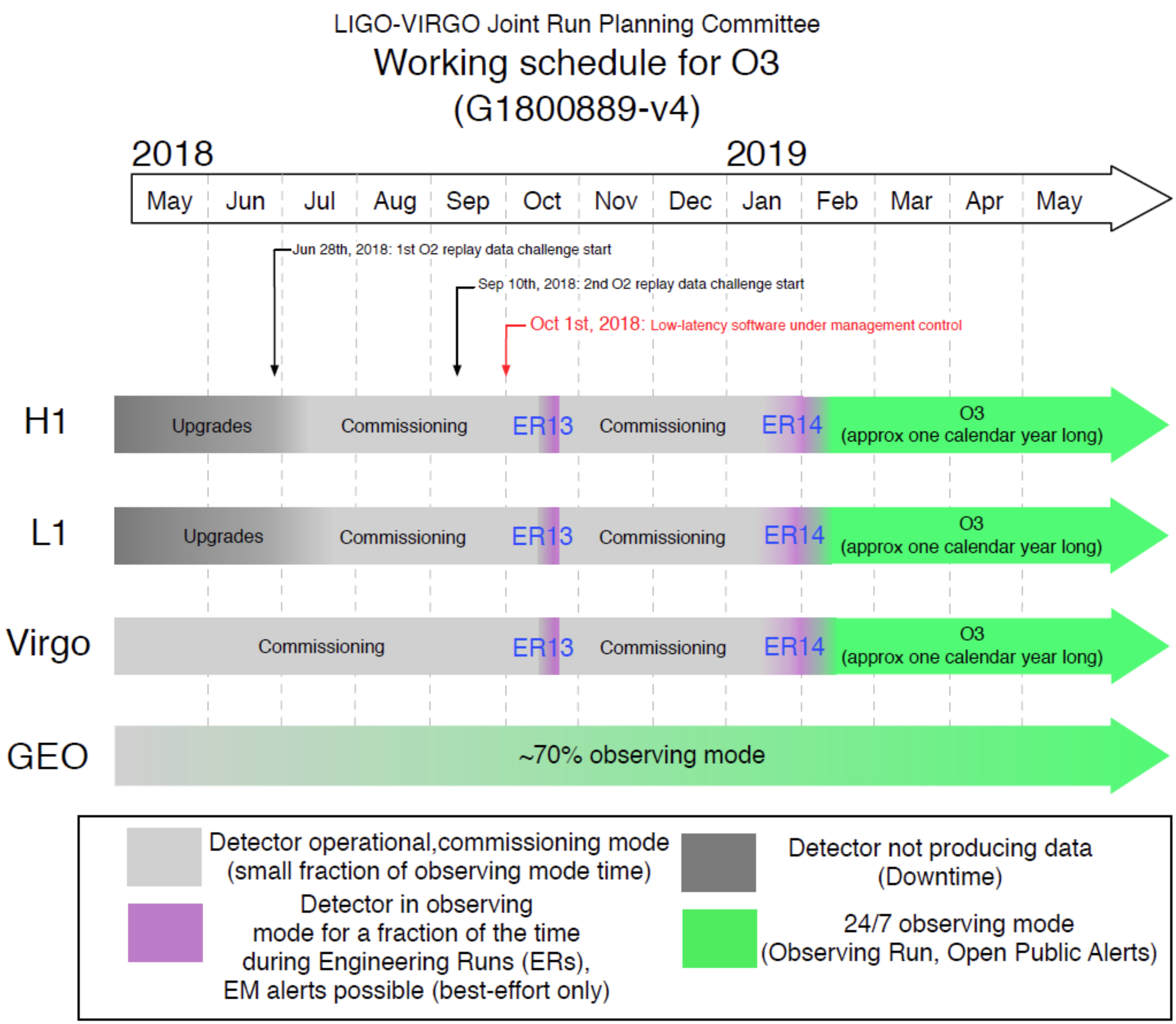
LIGO-VIRGO Joint Run Planning Committee
Working schedule for O3
(G1800889-v4)
2018
2019
May
Jun
Jul
Aug
Sep
Oct
Nov
Dec
Jan
Feb
Mar
Apr
May
Jun 28th, 2018: 1st O2 replay data challenge start
Sep 10th, 2018: 2nd O2 replay data challenge start
Oct 1st, 2018: Low-latency software under management control
H1
Upgrades
Commissioning
ER13
Commissioning
ER14
O3
(approx one calendar year long)
L1
Upgrades
Commissioning
ER13
Commissioning
ER14
O3
(approx one calendar year long)
Virgo
Commissioning
ER13
Commissioning
ER14
O3
(approx one calendar year long)
GEO
~70% observing mode
Detector operational,commissioning mode
(small fraction of observing mode time)
Detector not producing data
(Downtime)
Detector in observing
mode for a fraction of the time
during Engineering Runs (ERs),
EM alerts possible (best-effort only)
24/7 observing mode
(Observing Run, Open Public Alerts)

FUTURE PERSPECTIVES

Medium and long term plans

LIGO-VIRGO-KAGRA OBSERVING SCENARIO

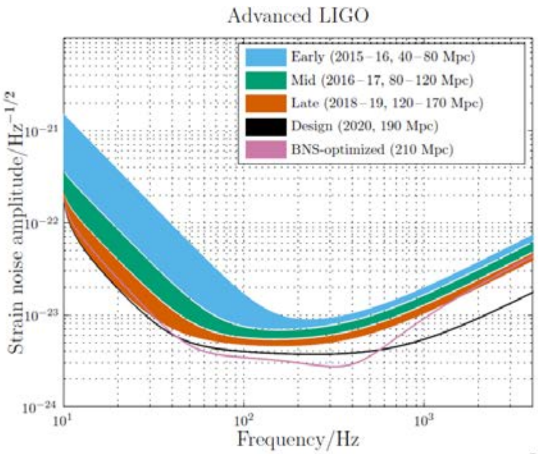

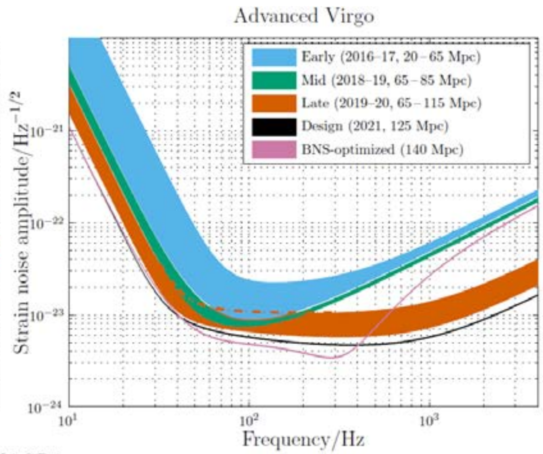

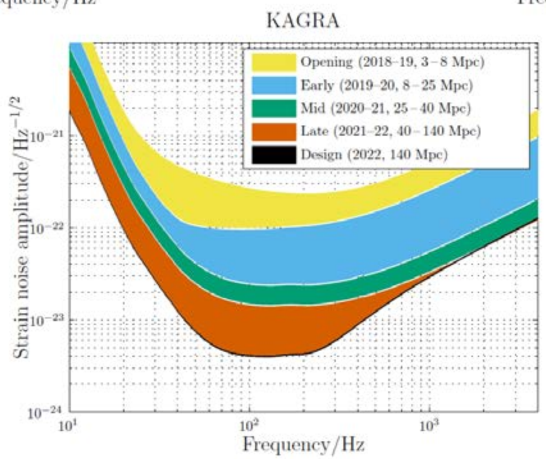

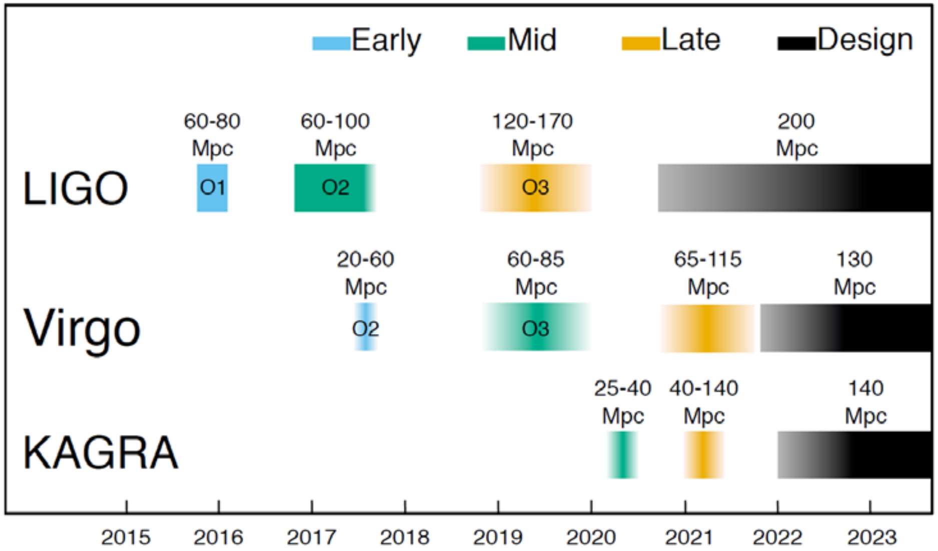

arXiv:1304.0670
Living Rev Relativ (2016) 19

THE CASE FOR BETTER DETECTORS

Number of events ∝ (Range)^3 × (Observation Time)

1 day of data at a range of 60 Mpc (projected O3) is equivalent to 125 days at 12 Mpc (initial-Virgo best)

Observing for a long time is good, improving the sensitivity is better

WHAT NEXT?

2.5 G: a set of upgrades capable of enhancing the sensitivities of the current detectors (event rate 5-10x)
AdV+ in Europe; A+ in USA

- Timeline: ~2024
- Cost: ~20Ú30 M€

3 G: new infrastructures/detectors capable of reaching the early universe. One order of magnitude gained in sensitivity wrt 2G

- Timeline: ~2030
- Cost > 1 G€

Einstein Telescope: European project for a nested assembly of 6 co-located interferometers, 10 km long

- underground
- bandwidth extended to 1 Hz
- cryogenics

Cosmic Explorer: US project for a 40 km interferometer

AdV+

Bridge to future 3G GW **astrophysics, cosmology, and nuclear physics**
Stepping stone to **3G detector technology**
Can be observing within **6 years** (2024)

Upgrades split in two phases:

Phase 1: BNS range up to 160 Mpc
– frequency dependent squeezing
– newtonian noise cancellation

Phase 2: BNS range up to 260 (300) Mpc
– new, larger mirrors
– new suspensions
– factor 3 of coating thermal noise reduction

ADVANCED VIRGO+ PHASE I

- Complete the AdV program:
  - 200 W laser; 125W at the ITF input
  - Signal recycling → 120 Mpc
- Frequency dependent squeezing
  - →150 Mpc
  - New filtering cavity

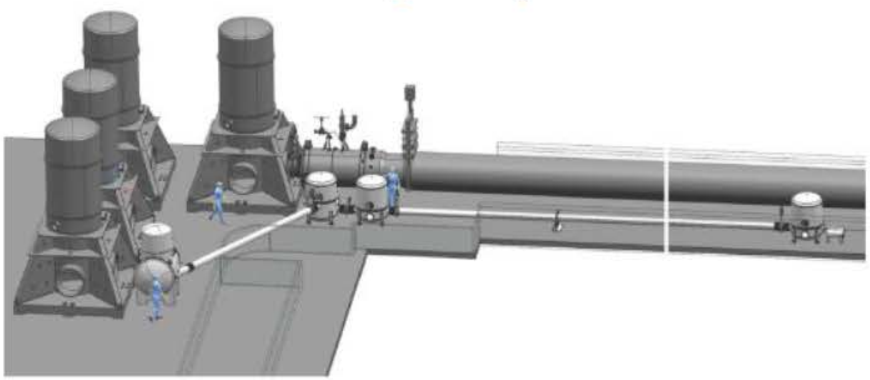

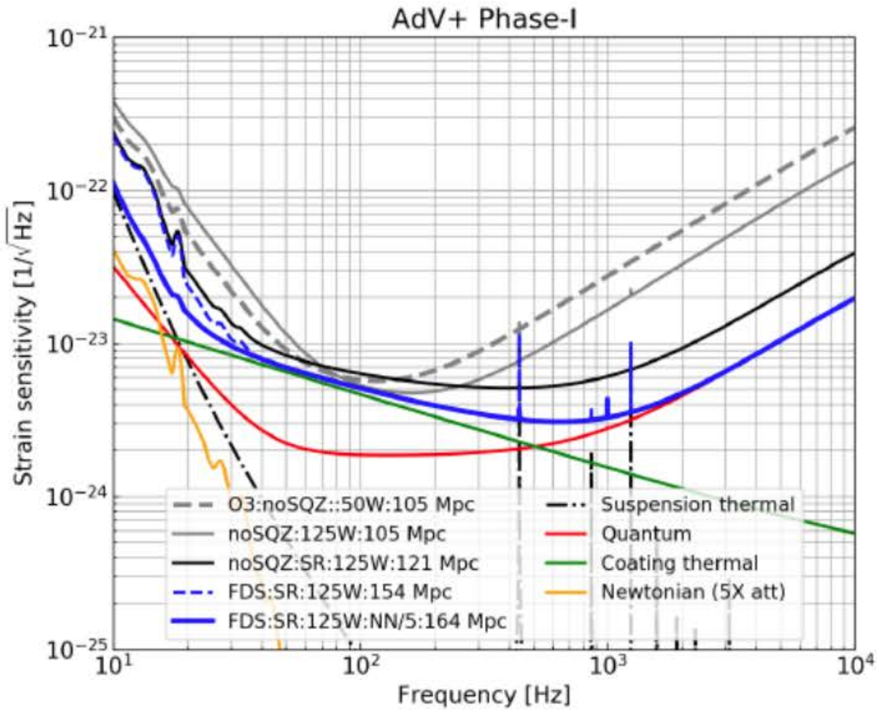

- Newtonian noise cancelation →160 Mpc

ADVANCED VIRGO+ PHASE II

- Larger mirrors
  - Diameter: 550 mm, thickness: 200 mm, mass: 105 kg (?)
  - Scenario 1: ETM-only → 200 Mpc
  - Scenario 2: full upgrade → 230 Mpc
- Coating improvements
  - If factor three reduction in CTN:
    - Scenario 1: ETM-only → 260 Mpc
    - Scenario 2: full upgrade → 300 Mpc
- Many challenges and activities
  - Grand Coater upgrade
  - Vacuum, infrastructure
  - Payloads and superattenuators
  - Aberration control

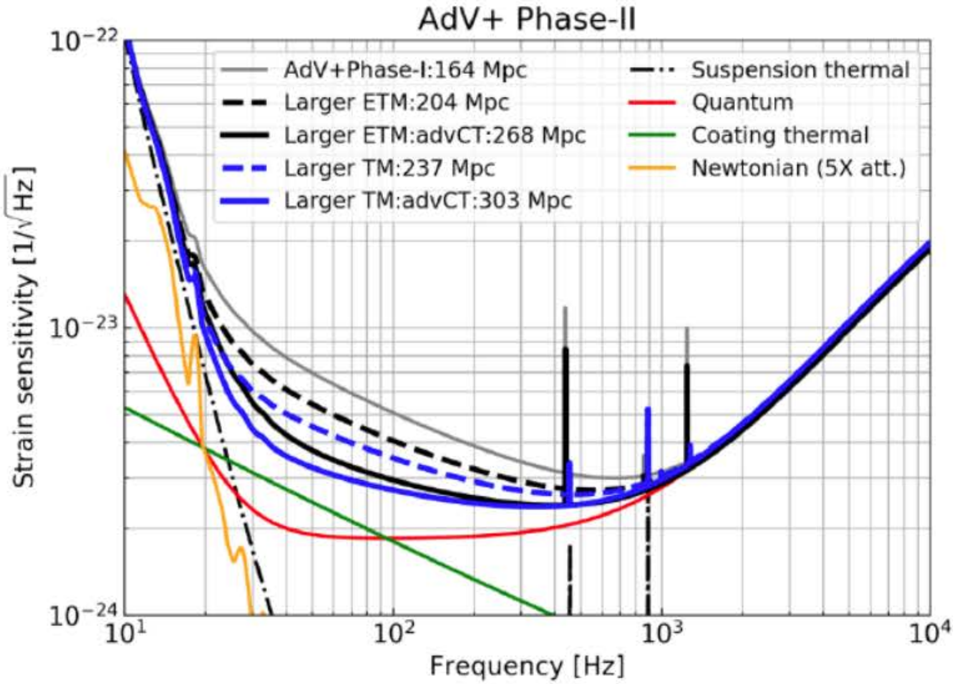

TENTATIVE TIMELINE

Five year plan for observational runs, commissioning and upgrades

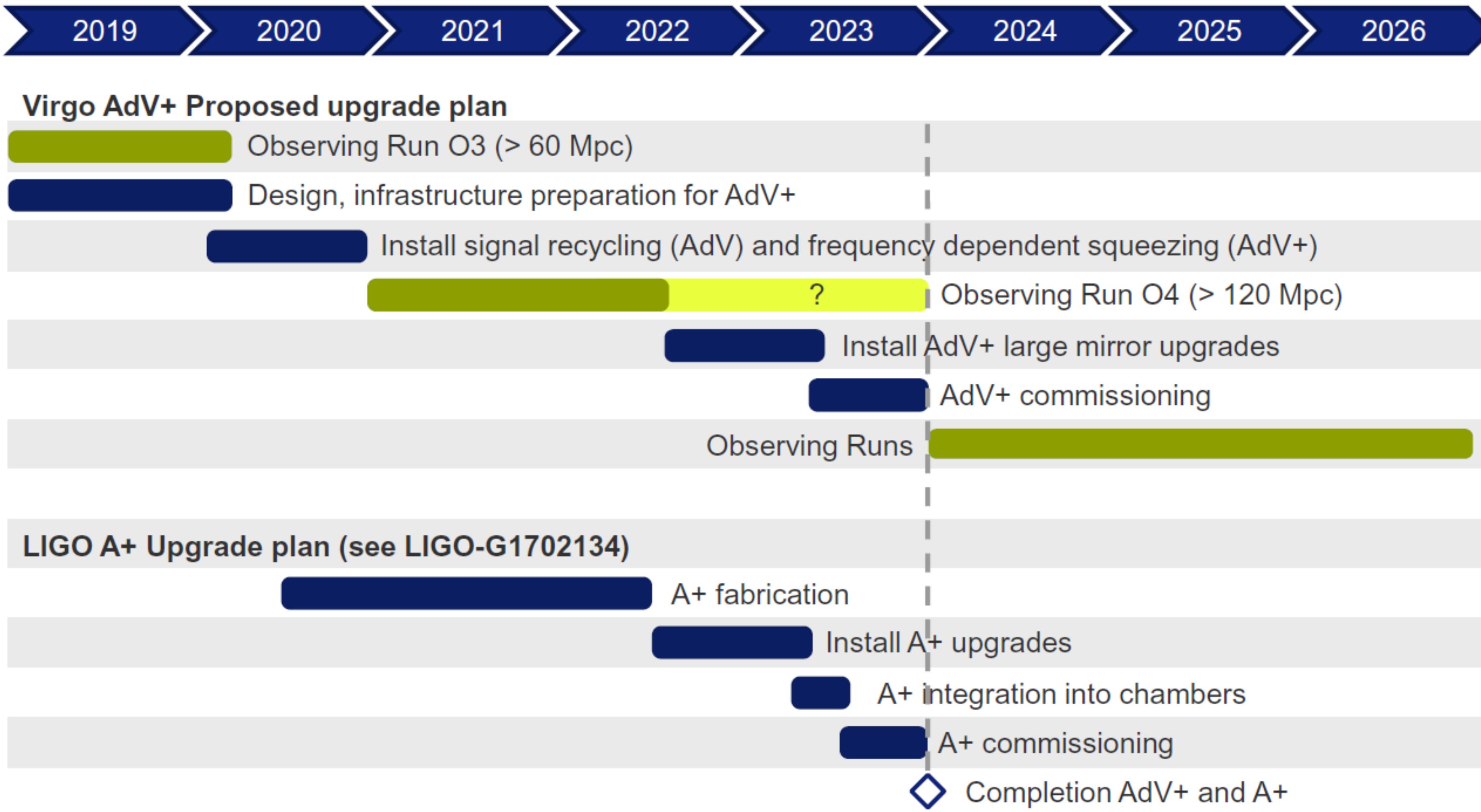

Note: duration of O4 has not been decided at this moment

TOWARDS A GLOBAL GW RESEARCH INFRASTRUCTURE

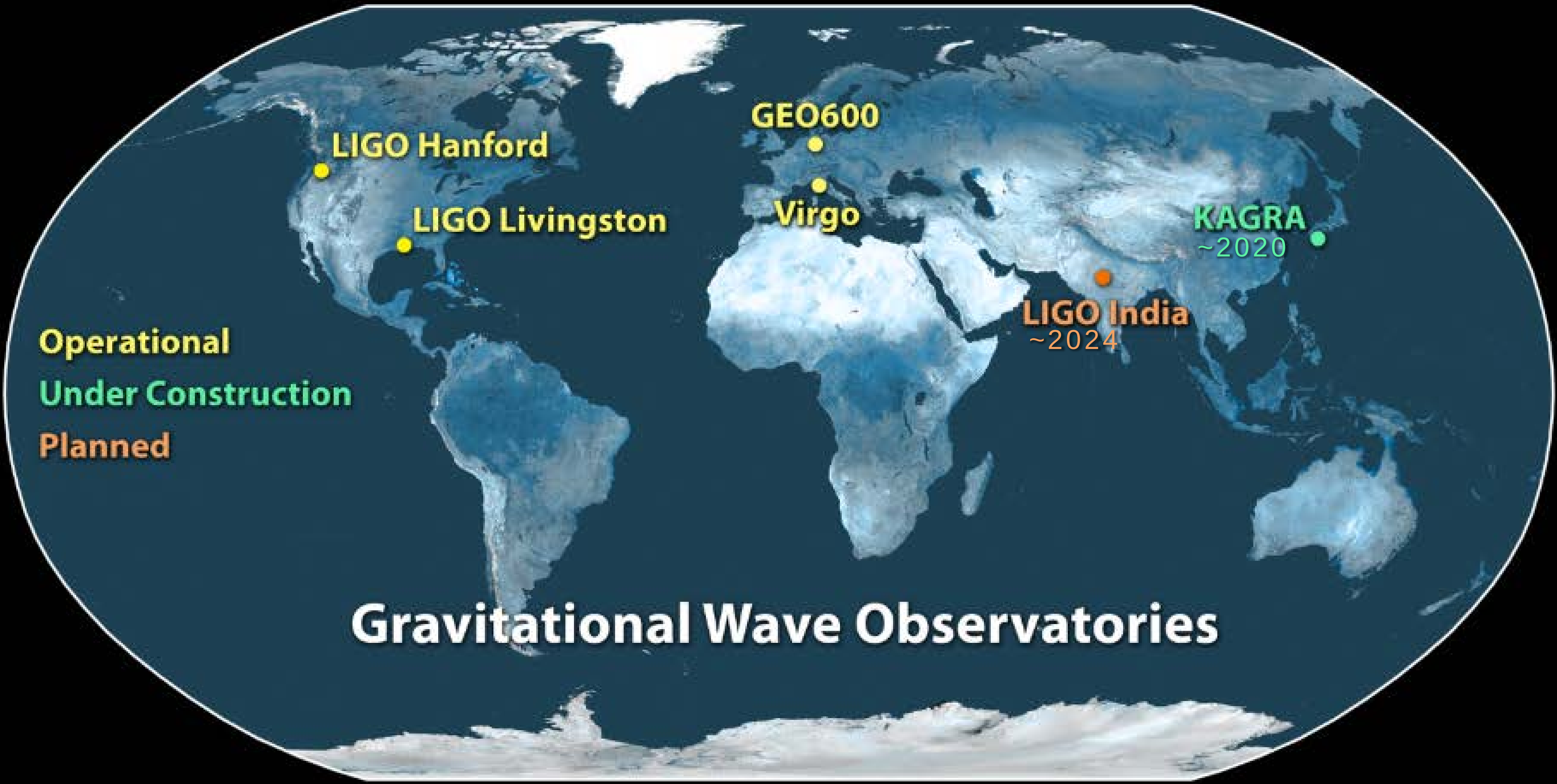

THE NETWORK IS THE DETECTOR

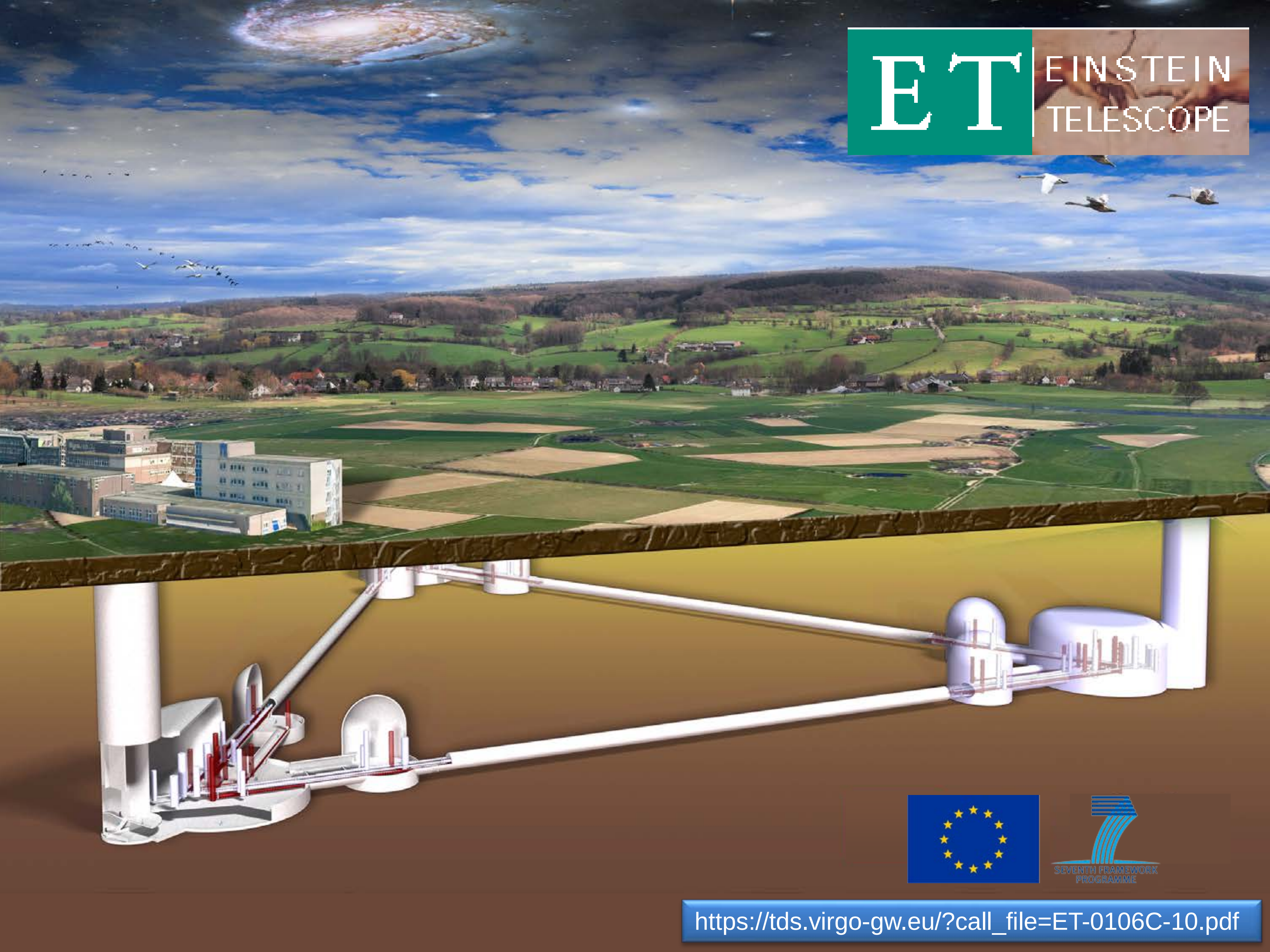
ET
EINSTEIN
TELESCOPE
SEVENTH FRAMEWORK
PROGRAMME
https://tds.virgo-gw.eu/?call_file=ET-0106C-10.pdf